Competitive and mutualistic dependencies in multispecies vegetation dynamics enabled by hydraulic redistribution

Juan C. Quijano,[1] Praveen Kumar,[1] Darren T. Drewry,[2,3] Allen Goldstein,[4] and Laurent Misson[4,5]

Received 17 September 2011; revised 9 February 2012; accepted 21 March 2012; published 11 May 2012.

[1] The goal of this study is to understand the interaction between belowground and aboveground ecohydrologic dynamics as facilitated by hydraulic redistribution. We analyze the partitioning of moisture and energy between tall and understory vegetation, and soil evaporation. Both the competitive and facilitative dependencies are examined using a shared resource model where the soil serves as a common reservoir for the interaction between the different vegetation species. The moisture state of the reservoir is altered by the addition and withdrawal by vegetation roots in conjunction with soil-moisture transport. Vertical patterns of soil moisture state and uptake reflect the nonlinear interactions between vegetation species. The study is performed using data from the Blodgett Forest Ameriflux site in the Sierra Nevada Mountains of California. The Mediterranean climate of the region, with wet winters and long dry summers, offers an ideal environment for the study. The results indicate that deep layer uptake of water by the tall vegetation and its release in the shallow layers enhances the productivity of the understory vegetation during the summer. The presence of understory vegetation reduces direct soil-evaporative loss making more moisture available for vegetation which enhances the total ecosystem productivity. The litter layer is also found to play an important role in the partitioning of the water and energy fluxes by damping the radiation reaching the soil and thereby reducing water loss due to soil evaporation.

Citation: Quijano, J. C., P. Kumar, D. T. Drewry, A. Goldstein, and L. Misson (2012), Competitive and mutualistic dependencies in multispecies vegetation dynamics enabled by hydraulic redistribution, *Water Resour. Res.*, *48*, W05518, doi:10.1029/2011WR011416.

1. Introduction

[2] The dynamics of water flow between plant roots and the surrounding soil play an important role in controlling the link between aboveground ecophysiological processes governing carbon, water and energy exchange, and the atmosphere [*Bardgett and Wardle*, 2010]. At longer timescales, these processes contribute to the formation of soil structure and the distribution of carbon and nutrients through the soil column [*Allton et al.*, 2007; *Angers and Caron*, 1998; *Huxman et al.*, 2004]. The flow of water from the roots to soil was first established experimentally by *Kramer* [1933], and has since been identified in a wide variety of plant species including shrubs [*Richards and Caldwell*, 1987; *Ryel et al.*, 2002; *Prieto et al.*, 2010], grasses [*Schulze et al.*, 1998] and trees [*Burgess et al.*, 1998; *Smith et al.*, 1999; *Burgess et al.*, 2000; *Brooks et al.*, 2006] across a range of dry to wet climates. The conductivities of transport through the root system are significantly larger than that of the surrounding soil [*Blizzard*, 1980], resulting in movement of moisture at rates that are substantially larger than those through the soil matrix [*Amenu and Kumar*, 2008]. As a result, the roots serve as preferential pathways for the movement of moisture from wet to dry soil layers. This passive transport is determined by the soil water potential gradients and can result in the transport of moisture deeper in the soil column during the wet season (hydraulic descent, HD) [*Burgess et al.*, 1998; *Schulze et al.*, 1998; *Smith et al.*, 1999; *Hultine et al.*, 2003], and transport of moisture from deep to shallow layers during the dry seasons (hydraulic lift, HL) [*Dawson*, 1993; *Espeleta et al.*, 2004; *Ishikawa and Bledsoe*, 2000; *Ludwig et al.*, 2003]. There is also evidence that roots can transport moisture laterally when a strong gradient in soil water potential is imposed across the breadth of a plant root system [*Brooks et al.*, 2002, 2006; *Nadezhdina et al.*, 2010]. This general phenomena of moisture transport through the soil system by way of the root system has been referred to as hydraulic redistribution (HR) [*Burgess et al.*, 1998, 2000, 2001; *Hultine et al.*, 2003, 2004].

[3] A number of studies have attempted to characterize the hydrologic and ecological significance of HR. The roles

[1]Department of Civil and Environmental Engineering, University of Illinois at Urbana-Champaign, Urbana, Illinois, USA.
[2]Max-Planck-Institut für Biogeochemie, Jena, Germany.
[3]Now at Jet Propulsion Laboratory, California Institute of Technology, Pasadena, California, USA.
[4]Department of Environmental Science, Policy, and Management, University of California at Berkeley, Berkeley, California, USA.
[5]Deceased 5 March 2010.

0043-1397/12/2011WR011416

of HR include buffering against daily soil water depletion and seasonal drought [*Emerman and Dawson*, 1996; *Bleby et al.*, 2010], facilitation of savanna tree-shrub clusters [*Zou et al.*, 2005], root litter decomposition and nutrient acquisition [*McCulley et al.*, 2004], extension of the growing season [*Ryel et al.*, 2002; *Scott et al.*, 2008], impact on competition between different plant functional types at continental scales [*Wang et al.*, 2010] and even alteration of seasonal climate [*Lee et al.*, 2005]. Although a number of species across a range of climate gradients from the tropical Amazon to the semiarid southwestern United States have been studied in this context, a predictive modeling based characterization that develops a comprehensive understanding of the impact of HR on the biophysical processes occurring in ecosystems with different species that coexist and share resources remains an open challenge.

[4] The objective of this study is to understand the role of HR in the interaction of aboveground and belowground ecohydrologic dynamics using a modeling approach. Specifically we explore the role of HR in regulating the partitioning, and trade-off of hydrologic fluxes between tall and understory vegetation and soil evaporation. This is accomplished using a "shared resource model" where the soil serves as a common reservoir whose state is altered by the addition and withdrawal of moisture by vegetation roots, in conjunction with the moisture transport dynamics and the nonlinear dependence of vegetation uptake and release on the existing soil-moisture state. The model extends the work of *Amenu and Kumar* [2008] for root and soil interactions through HR for a single species to incorporate moisture uptake and release dynamics involving roots of multiple plant species. It also extends the model of *Drewry et al.* [2010a, 2010b] developed for coupling the belowground moisture transport through soils and root system, and aboveground water, energy, and carbon fluxes for both C3 and C4 vegetation to allow for multispecies composition of vegetation. Further, the existing functional representation of HR is enhanced to represent ecosystem scale dependencies such as soil evaporation and its dependency on the litter layer.

[5] Both hydraulic descent and lift affect soil evaporation. *Ryel et al.* [2002] suggested that by transporting water down to deeper layers, hydraulic descent reduces the moisture that would otherwise be available for soil evaporation. On the other hand hydraulic lift may allocate water to shallow layers that is likely to support evaporation [*Dawson*, 1993, 1996] which could be detrimental for the plants in water-limited environments. In some cases water potential in the soil can reach very low levels thereby creating a soil-root potential gradient for the movement of significant volume of moisture from the roots into the soil. It has been suggested that in such conditions it is likely that physiological controls may act to reduce the efflux of water [*Caldwell et al.*, 1998; *Jackson et al.*, 2000; *Espeleta et al.*, 2004], for example through the death [*Espeleta et al.*, 2004] or shrinkage [*Jackson et al.*, 2000] of fine roots near the ground surface. We explore this situation by implementing a hydraulic fuse mechanism [*Espeleta et al.*, 2004], which is a hydraulic disconnection between roots and the surrounding soil when the daily average water-potential in the soil falls below the wilting point, thereby preventing both uptake and release of water by the roots. On the other hand the presence of a litter layer lying over the soil has been observed to influence the energy balance at the surface. Experimental and numerical studies have recognized that the presence of a litter layer above the soil reduces evaporative fluxes [*Park et al.*, 1998; *Bristow et al.*, 1986; *Bussiere and Cellier*, 1994; *Chung and Horton*, 1987] and soil temperature [*Bussiere and Cellier*, 1994; *Chung and Horton*, 1987]. Therefore, the presence of litter introduces a new level of complexity that impacts the dynamics occurring belowground. Here we also analyze how the presence of litter influences the subsurface transport of moisture by HR through the regulation of soil evaporation.

[6] The role of water uptake and its redistribution is of significant interest at the ecosystem scale [*Scott et al.*, 2008]. Although important advances have been made in detecting the presence of HR and the quantification of the moisture fluxes it produces [*Caldwell et al.*, 1998; *Yoder and Nowak*, 1999; *Burgess et al.*, 1998; *Domec et al.*, 2010; *Wang*, 2011], most studies have been conducted to understand its significance on the transpiration and gross productivity of a single plant species [*Caldwell and Richards*, 1989; *Brooks et al.*, 2002; *Ryel et al.*, 2002], or have considered a lumped system that encapsulates the net impact of species composition [*Amenu and Kumar*, 2008] rather than resolving the competitive or mutualistic dependencies between different species. Although the presence of more than one species sharing the soil and resources, such as water and nutrients, in the same ecosystem imply competition for resources, there is experimental evidence that also suggests that facilitation of shared resources between different species may occur [*Ludwig et al.*, 2003; *Scott et al.*, 2008]. It has also been suggested that HR may influence the dynamics of microbial populations and consequently the biogeochemical cycling [*Caldwell and Richards*, 1989; *Caldwell et al.*, 1998; *McCulley et al.*, 2004; *Querejeta et al.*, 2007] resulting in a mutual feedback effect between vegetation and microbial populations in the soil. These studies have established HR as a significant ecohydrological process with implications for ecosystem dynamics and the interactions between vegetation and the atmosphere. Model and simulation studies present an opportunity to further unravel the complexity of these ecohydrological processes and their role in ecosystem functioning [*Kumar*, 2011]. Here we use a novel process-based model, capable of incorporating HR in a multispecies framework, to gain deeper insight into ecosystem scale hydrological dynamics and interactions. In particular, we explore how the presence of multiple species utilizing the same soil domain induces both competitive trade-off in water utilization and mutualistic benefits in ecosystem productivity, and the role of HR in mediating these interactions. The impact of these processes on subsurface nutrient dynamics is presently being studied.

[7] In section 2 we describe the Blodgett Forest study site. The shared resource model developed for this study is described in section 3. Results and analyses for aboveground and belowground hydrologic fluxes and states is presented in section 4. Section 5 provides a summary and discussion of the key points. A list of symbols is included in the notation section and several technical aspects of the model are presented in the Appendix A–C.

2. Study Site

[8] The Ameriflux study site in the Blodgett Forest was established in 1997 in the Sierra Nevada Mountains in California, United States (38.8952°N, 120.6328°W, 1315 m above MSL) [*Goldstein et al.*, 2000]. In 1997 the ground cover consisted of 25% shrubs, 30% conifer trees, 2% deciduous trees, 7% forbs, 3% grasses and 3% stumps [*Fisher et al.*, 2005]. The dominant overstory species is *Pinus Ponderosa* (hereafter PP) and the most ubiquitous understory shrubs are *Arctostaphylos manzanita* and *Ceanothus Cordulatus* (hereafter shrubs) [*Xu and Qi*, 2001; *Misson et al.*, 2006]. The region is characterized by a Mediterranean climate with wet winters and long dry summers in which most of the precipitation falls between September and May with little rainfall between June and October. PP is a native forest species in the western regions of North America which has adapted to the long dry summers in California and the Pacific Northwestern United States [*Panek*, 2004]. PP trees are able to sustain high transpiration rates during the dry period [*Panek*, 2004]. Observational studies have demonstrated the presence of HR in PP [*Brooks et al.*, 2002; *Domec et al.*, 2004; *Warren et al.*, 2007], indicating that hydraulically lifted water provides a substantial portion of dry-season transpiration in these deep-rooted trees.

[9] Ponderosa pine was initially planted at the Blodgett Forest site in 1990 [*Tang et al.*, 2005]. At the end of the 1998 growing season the leaf area index (*LAI*) of overstory (total needle surface area) and understory (total surface area) vegetation was about 4.5 and 1.6, respectively [*Xu and Qi*, 2001]. In June of 1999 most of the shrubs were removed and in the spring of 2000 the PP plantation was thinned in order to analyze variations in carbon flux due to management practices [*Misson et al.*, 2005]. The *LAI* reduction after the thinning was around 30% [*Xu and Qi*, 2001]. PP was the predominant species in 2001 but in 2002 the shrubs returned. The *LAI* trends for the shrubs and the pines are shown in Figure 1 (note zero *LAI* for the shrubs in 2001) along with ecophysiological parameters V_{cmax} and J_{max} [*Farquhar et al.*, 1980]. Figure 1 also shows the seasonal rainfall and incoming shortwave radiation patterns, where the signature of the Mediterranean climate is clearly evident.

[10] These site and climate characteristics provide for an ideal environment to study the role of HR and multispecies interactions. Simulations for 2001 involving only PP and for 2002 involving PP and shrubs allow us to compare and contrast the single and multispecies response. Shrubs started to grow back in 2002 but the maximum *LAI* of 1 reached during 2002 is low compared with the maximum value of 2 reached in 1998 [*Goldstein et al.*, 2000] before they were cut. This suggest that the shrubs had not fully established in 2002. The parameters for the model described in section 3 are obtained from published literature and listed in Tables 1 and 2. In most cases they were measured directly at the Blodgett Forest site. The data for year 2000 are used for model spin-up by running the model several times consecutively with this 1 year of data until the annual cycle of soil moisture reaches steady state. Each scenario (see section 4) is spun up independently using year 2000 forcing data, resulting in different initial conditions for the start of each simulation experiment, which spanned the study period 2001–2002.

3. Shared Resource Model for Multiple Species Interactions

[11] The model development is based upon the multilayer canopy-soil-root (MLCan) biophysical model of *Drewry et al.* [2010a, 2010b]. MLCan incorporates explicit coupling between leaf-level ecophysiological processes (photosynthesis and stomatal conductance), physical processes (energy balance and boundary layer conductance), and belowground water status which incorporates the HR model of *Amenu and Kumar* [2008]. It resolves the radiation regimes, both direct and diffuse shortwave as well as longwave, throughout the vertical domain of the canopy. Radiation attenuation is determined by the leaf area density (*LAD*) profile [*Drewry et al.*, 2010a]. It predicts the latent and sensible heat fluxes for each canopy layer through an iterative solution of the leaf energy balance, considering sunlit, shaded, and wet leaf fractions (due to dew or rainfall interception) separately. CO_2 fluxes (assimilation and respiration) are also calculated for each canopy layer, being directly coupled to the energy balance through stomatal dynamics. The details of the MLCan formulation can be found in the online supplement of *Drewry et al.* [2010a].

[12] For this study, the MLCan model is extended to include formulations for several plant species coexisting in the same environment. As the MLCan model is designed to include both C3 and C4 photosynthetic pathways, it allows us to study the interaction between different tall and understory vegetation combinations: C3-C3, C3-C4 (or in rare cases C4-C4). This enables us to simulate the water, energy, and carbon dynamics when several species with different structural and ecophysiological characteristics interact and share resources. The role of HR in these interactions is of particular interest in this study.

[13] The schematic of the model is presented in Figure 2. As illustrated, we assume that several species can coexist in the same environment and they are homogeneously distributed in the spatial domain. Aboveground, their coexistence affects the radiation regime. For example, tall vegetation can shade the understory vegetation, thus reducing the radiation available for understory plants. Radiative effects such as this will directly impact the partitioning of energy between ecosystem components, the energy balance of each vegetation type and the soil, and consequently the net photosynthetic productivity of the system. The different rooting depths and root distributions of tall and understory vegetation impact belowground resource acquisition, as different species draw from the same resource pool, but potentially with different strengths and from different locations in the soil profile.

[14] We assume that all the individuals of a given species have the same structural and ecophysiological characteristics, but each plant species is different from the other. To resolve the light regime we use a composite *LAD* obtained as a linear sum of the *LAD* of the individual species. This composite *LAD* is then used to attenuate the transmission of downward radiation. Once the light attenuation is solved, the energy absorbed by the canopy at different layers is obtained using a weighted average calculation based on the fraction of *LAD* from each species in the composite *LAD* at each layer (see equation (A4)). This approach allows us to separately consider the ecophysiological and structural

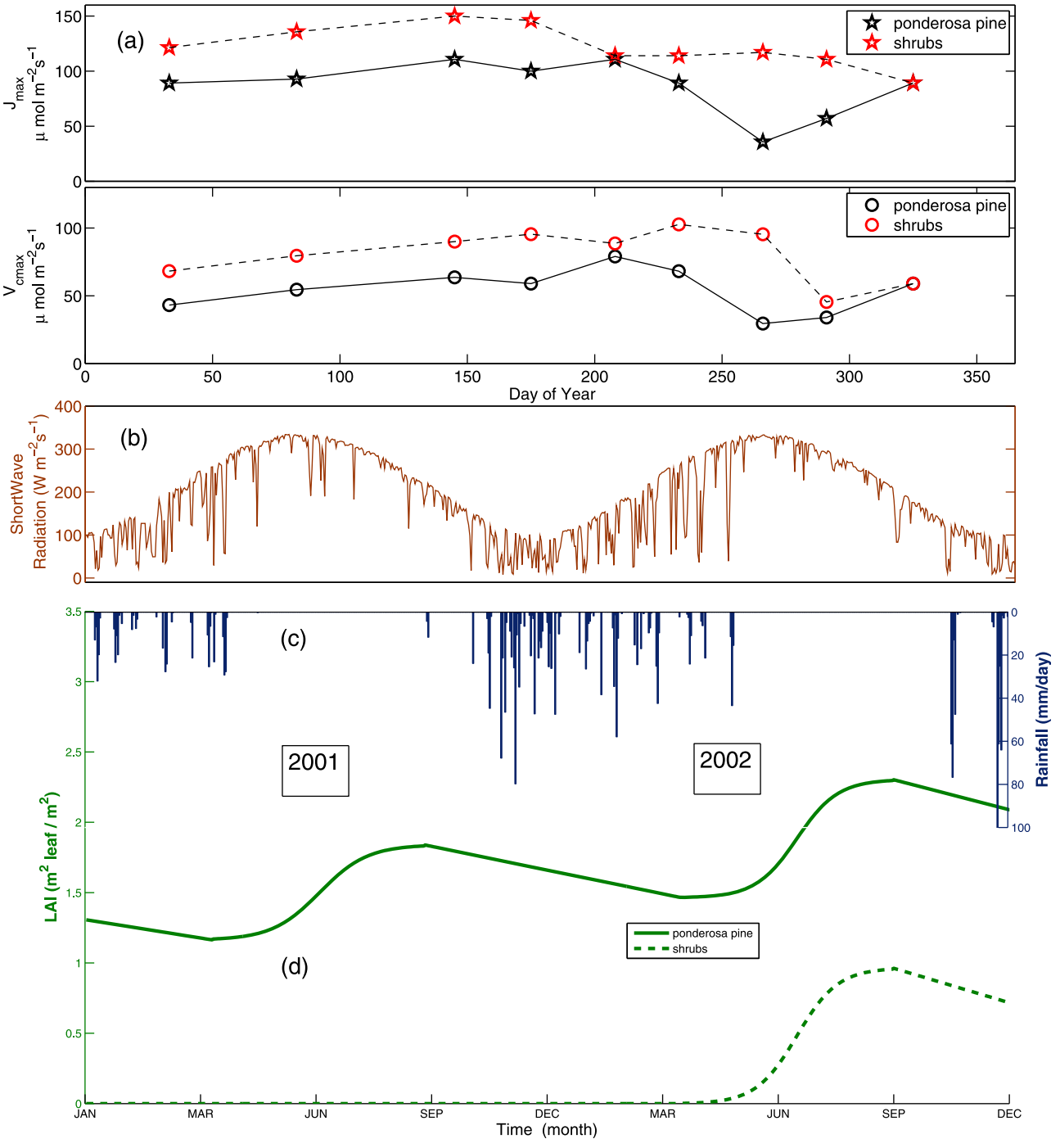

Figure 1. Physiological and climatological data from Blodgett used in the model simulations. (a) Variation of maximum rate of electron transport (J_{max}) and maximum carboxylation velocity (V_{cmax}) throughout the year (data obtained from *Misson et al.* [2006]). (b) Daily averaged downward shortwave radiation, (c) rainfall for 2001 and 2002, and (d) leaf area index (LAI). All-sided ponderosa pine *LAI* is 2.3 times *LAI* shown (projected). (*LAI* data obtained from *Misson et al.* [2005]).

differences of each species. As a result, the latent heat, sensible heat, and CO_2 flux profiles for each species are different.

[15] The HR dynamics are formulated by extending the single species model of *Amenu and Kumar* [2008] and *Mendel et al.* [2002], which are based on coupling two equations for the transport of moisture through the soil and the root system. The presence of M different plant species necessitates the use of M independent equations for the transport of moisture through the root systems. This allows for their differences in structural and functional properties to be incorporated. These root system equations are coupled

Table 1. List of Parameters Used in the Simulations for the Blodgett Site

Description	Symbol	Units	Ponderosa Pine	Shrubs
Photosynthesis				
Fraction absorbed Q available to photosystem II	B_f	–	0.5[a]	0.5[a]
Conductance and Leaf States				
Ball Berry slope	m	–	13[b]	13
Ball Berry intercept	b	$\frac{\text{mol}}{\text{m}^2\text{s}}$	0.001[c]	0.001[c]
Stomatal sensitivity parameter for m	s_f	MPa^{-1}	1[b]	1
Ψ_l at which half potential for m is lost	Ψ_f	MPa	−2[b]	−2
Leaf forced convection parameter	c_f	–	4.3×10^{-3} [d]	4.3×10^{-3}
Leaf free convection parameter	c_f	–	1.6×10^{-3} [d]	1.6×10^{-3}
Canopy Structural				
Canopy Height	hc	m	5[e]	1[e]
Displacement Height	d	m	2/3 hc	2/3 hc
Leaf width (Needle diameter)	do	m	0.001[f]	0.02[g]
Shoot diameter for Conifers	wo	m	0.07[f]	–
Maximum H_2O storage capacity of a leaf	S_m	$\frac{\text{mm}}{(\text{LAI})}$	0.2	0.2
Foliage drag coefficient	C_d	–	0.5[h]	0.5[h]
Mixing Length coefficient	α	–	0.13[h]	0.13[h]
Decay Coefficient for Leaf Nitrogen Content	k_n	–	0.5	0.5
Radiation and Energy Balance				
Leaf emissivity	ϵ_l	–	0.95[i]	0.95
Leaf Reflectance in the Visible Wavelength	ϵ_{rv}	–	0.09[f]	0.09
Leaf Transmittance in the Visible Wavelength	ϵ_{rt}	–	0.06[f]	0.06
Leaf Reflectance in the near IR Wavelength	ϵ_{ri}	–	0.52[f]	0.52
Leaf Transmittance in the near IR Wavelength	ϵ_{ti}	–	0.35[f]	0.35
Leaf angle distribution parameter	x	–	0.6[j]	0.6
Root Structure				
Maximum Root depth	r_d	m	10	0.85
Fiftieth percentile rooting depth Logistic Equation	z_{50}	m	0.37[k,l]	0.07[k]
Ninety-fifth Percentile Rooting Depth Logistic Equation	z_{95}	m	2.60[k,l]	0.48[k]
Radial Conductivity	K_{rad}	s^{-1}	5.0×10^{-8}[k,l,m]	2.5×10^{-8}[k,l,m]
Axial Conductivity	K_{ax}	$\text{mm}^2\ \text{s}^{-1}$	0.2[k,l,m]	0.1[k,l,m]

[a] *Bernacchi et al.* [2003], *Bernacchi et al.* [2005].
[b] *Misson et al.* [2004]. See also Appendix B.
[c] From sensitivity analysis.
[d] *Nikolov* [1995].
[e] *Fisher et al.* [2007].
[f] *Kurpius et al.* [2003].
[g] *Smith* [2005].
[h] *Katul et al.* [2004].
[i] *Campbell and Norman* [1998].
[j] Assuming more tendency toward vertical leaf angle distribution [*Schade*, 2002].
[k] *Jackson et al.* [1997].
[l] *Amenu and Kumar* [2008].
[m] *Huang and Nobel* [1994].

with a single Richards equation for soil-moisture transport through the soil profile. The system of equations is

$$\begin{aligned}
&\frac{\partial\theta}{\partial t} - \frac{\partial}{\partial z}\left[K_s\left(\frac{\partial \psi s}{\partial z} - 1\right)\right] = -\sum_{i=1}^{M} K_{r_i}^R\left(\psi_s - \psi_{r_i}\right)\\
&-\frac{\partial}{\partial z}\left[K_{r_1}^A\left(\frac{\partial \psi_{r_1}}{\partial z} - 1\right)\right] = K_{r_1}^R\left(\psi_s - \psi_{r_1}\right)\\
&-\frac{\partial}{\partial z}\left[K_{r_2}^A\left(\frac{\partial \psi_{r_2}}{\partial z} - 1\right)\right] = K_{r_1}^R\left(\psi_s - \psi_{r_2}\right)\\
&\cdots\\
&-\frac{\partial}{\partial z}\left[K_{r_M}^A\left(\frac{\partial \psi_{r_M}}{\partial z} - 1\right)\right] = K_{r_M}^R\left(\psi_s - \psi_{r_M}\right)
\end{aligned}, \quad (1)$$

where the first equation is the Richards equation and the other M equations represent transport through M different plant species. The terms ψ_s and ψ_{r_i} are the water potential in the soil and the root of the ith plant species, respectively, and θ is the soil-moisture. The vertical coordinate and time are represented as z and t, respectively. Note that there is a unique water potential value for the roots of each plant species in each layer. The term K_s is the soil hydraulic conductivity, and $K_{r_i}^R$ and $K_{r_i}^A$ are the radial and axial root conductivities of the ith plant species, respectively [*Amenu and Kumar*, 2008]. These equations are solved simultaneously for 12 layers where central nodes are located at 0.7, 2.8, 6.2, 11.9, 21.2, 36.6, 62.0, 103.8, 172.7, 286.5, 474.0, 783.0 cm below the surface.

[16] The individual root systems of each species do not directly interact. They do share the common soil system, such that θ and ψ_s in each soil layer are the same for all

Table 2. List of Parameters for the Soil and Litter Model

Description	Symbol	Units	Value
Soil Parameters			
Atmospheric Emissivity	ϵ_a	–	0.94[a]
Soil Surface Emissivity	ϵ_s	–	0.85[a]
Litter Parameters			
Saturated Litter Moisture	θ_{Ls}	–	0.8[b]
Litter Moisture at Field Capacity	θ_{Lfc}	–	0.025
Litter Moisture at which r_s (resistance to *LE* due to litter) becomes zero	θ_{Lr}	–	0.2[c]
Litter Moisture at which evaporation (LE_{soil}) becomes negligible	θ_{Le}	–	0.0001
Exponent for Litter Matric Potential	b_l	–	2.42[d]
Matric Potential for Litter Moisturized at 1 kg kg^{-1}	ψ_{1l}	m	35.3[d]
Litter Thickness	Δz	cm	3
Litter Thermal Conductivity	TC_L	W m^{-1} K^{-1}	0.15[e]
Litter Thermal Diffusivity	α_L	m^2 s^{-1}	5.7×10^{-7}[e]

[a] *Campbell and Norman* [1998].
[b] *Park et al.* [1998].
[c] *Schaap et al.* [1997].
[d] *Ogee and Brunet* [2002].
[e] *Ahn et al.* [2009].

species (see Figure 2). This conceptualization of shared resource dynamics allows us to capture interspecies interactions, both competition and mutualism, as the water uptake or release by one species affects the shared soil moisture state, resulting in an indirect effect of each vegetation species on the dynamics of the others. When plants uptake water from the same layer they compete for available water. The release of water through hydraulic redistribution may, however, benefit the other species that share that layer by increasing available moisture. The model can simulate HR in all plant species and is structured so that the ability to hydraulically redistribute water can be switched off on a selective basis by setting the root radial conductivity of a species to zero, i.e., $K_{r_i} = 0$, when the water potential in the roots is higher than the water potential in the soil, i.e., $\psi_{r_i} > \psi_s$. This approach to simulate the impacts of HR has been used previously by *Mendel et al.* [2002].

[17] The maximum root distribution for shrubs during 2002 is unknown. *Ceanothus Cordulatus*, which accounts for 22% of the understory shrubs [*Fisher et al.*, 2007], are able to resprout from remnants of roots belowground [*Oakley et al.*, 2003]. *Arctostaphylos manzanita* comprise the remaining 78% of understory shrubs. They can reach up to 3 m in height after many years of establishment. However *Arctostaphylos manzanita* has difficulty in resprouting from remnants of belowground roots [*Peterson*, 1975; *Wright and Bailey*, 1982] and is mainly established from seeding. According to *Fisher et al.* [2007], shrubs reached 1 m height in 2003 and a maximum *LAI* of 1.6 which is close to the maximum *LAI* of 2 reported in 1998 before they were cut [*Goldstein et al.*, 2000]. This suggests that the shrubs were not fully established in 2002. Available information for *Arctostaphylos patula* shrubs in the Sierra Nevada region suggests that at full establishment the rooting depth can be up to 160 cm [*Plamboeck*, 2008]. For our study we have assumed a maximum rooting depth of 85 cm and performed sensitivity analyses for the range 60 cm to 140 cm and included in the discussion. The 50th (z_{50}) and 95th (z_{95}) percentile of the root depth for shrubs used in this study were obtained by scaling those reported in the work of *Schenk and Jackson* [2002]. The maximum root distribution for ponderosa pine was found to reach 10 m. However most of the root biomass is allocated in the first 2 m with z_{50} and z_{95} 0.37 m and 2.60 m, respectively [*Amenu and Kumar*, 2008].

[18] The MLCan model, thus modified to incorporate multiple species interactions, can be used to study the ecohydrologic consequences of the coexistence of multiple vegetation species. Our preliminary investigations with the MLCan model at the Blodgett Forest site indicated that the litter present on the soil surface could play a significant role in both the surface energy balance and the water balance of the system. *Ogee and Brunet* [2002] and *Wilson* [2000] have also emphasized the role of litter on the estimation of soil evaporation and energy balance. A litter layer can act to decrease the conductivity of water vapor between the soil surface and the atmosphere. This effect, therefore, reduces the latent heat flux (LE_{soil}) from the soil surface. Furthermore, the thermal conductivity of a litter layer is considerably smaller than that of the soil, causing the ground heat flux (G) to also be reduced. The net result of these effects is an increase in the sensible heat flux and emitted longwave radiation due to an increase in temperature at the surface.

[19] Given the potential importance of litter at the Blodgett Forest site, we have included a litter model for this study, which is described in Appendix B (see also Figure 3). Its implementation requires parameters such as the thickness, thermal conductivity, and thermal diffusivity, which are obtained from existing literature and are listed in Table 2.

[20] Throughout the study we contrast the impact of including or excluding a litter layer. Figure 4a shows the ground heat flux at the surface computed for the year 2001. The red and the blue lines show the predicted G at the surface when a litter layer is excluded and included, respectively. It can be seen that the incorporation of a litter layer has a significant impact on the magnitude of the ground heat flux. Figure 4b shows the same fluxes but now G is computed at 8 cm below the surface, a depth at which measured ground heat flux is available (black dots in Figure 4b). The simulation, when a litter layer is included, matches better the fluxes observed at the Ameriflux site. Also the

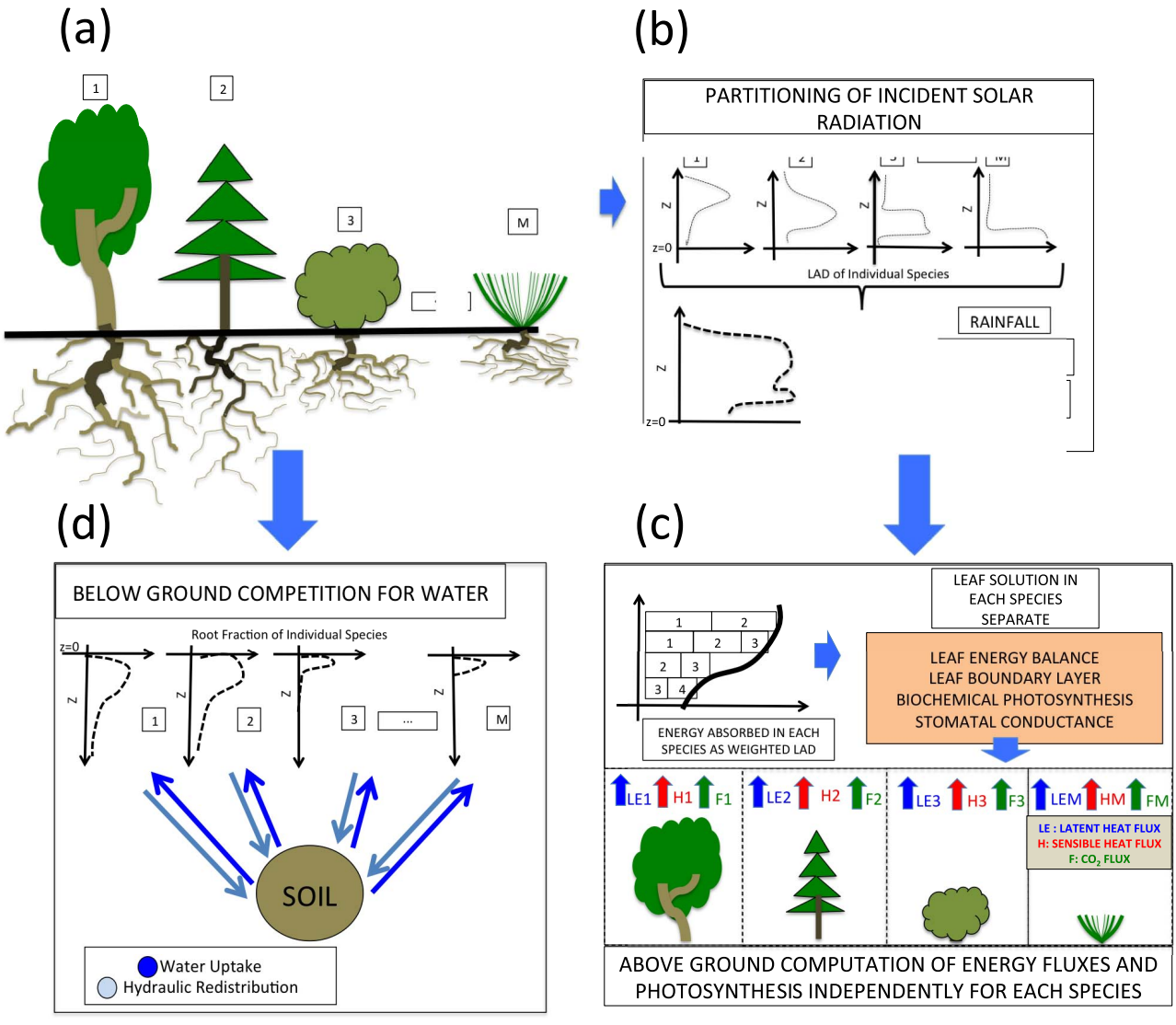

Figure 2. Schematic representation of the multispecies MLCan model. (a) The structure and composition of the above ground canopy involving several vegetation species determines the partitioning of the incident solar radiation and water uptake patterns. (b) The combination of the leaf area density (*LAD*) of each individual species is used to develop a compound *LAD*. This compound *LAD* in turn determines the radiation regime through the vertical profile and the radiation reaching the soil. (c) The energy absorbed or emitted by each species at different levels is a function of the fraction of the *LAD* of that species in the compound *LAD*. (d) Below the ground the uptake of water and nutrients by each species is coupled with a common soil pool. The model framework allows the incorporation of different ecophysiological and structural parameters for the vegetation species considered.

inclusion of the litter layer increases the release of sensible heat from the surface and decreases the release of latent heat (not shown). Figures 4c and 4d show the sensitivity of the ground heat flux to the litter layer thickness and the thermal conductivity, respectively. When the litter layer is thicker (Figure 4c) or the thermal conductivity is lower (Figure 4d) the ground heat flux decreases. The litter layer thickness is specified as 3 cm (which is within the range reported by *Black and Harden* [1995] at Blodgett), and the thermal conductivity is set as 0.15 W m^{-1} K^{-1} (which is within the range of values reported by *Ahn et al.* [2009]). Figures 4a and 4b are illustrated using these values.

4. Results and Analysis

4.1. Latent Heat Flux and Water Uptake

[21] The extraction of soil moisture to satisfy the transpirational demand is regulated by the interplay of different variables such as leaf phenology, vertical distribution of root biomass, ecophysiological properties and the available soil moisture. The contrasting characteristics of tall and understory vegetation will result in signature differences in soil water extraction in time and space, making their coupled dynamics complex, with the potential for both competitive and mutualistic interactions. In this section we

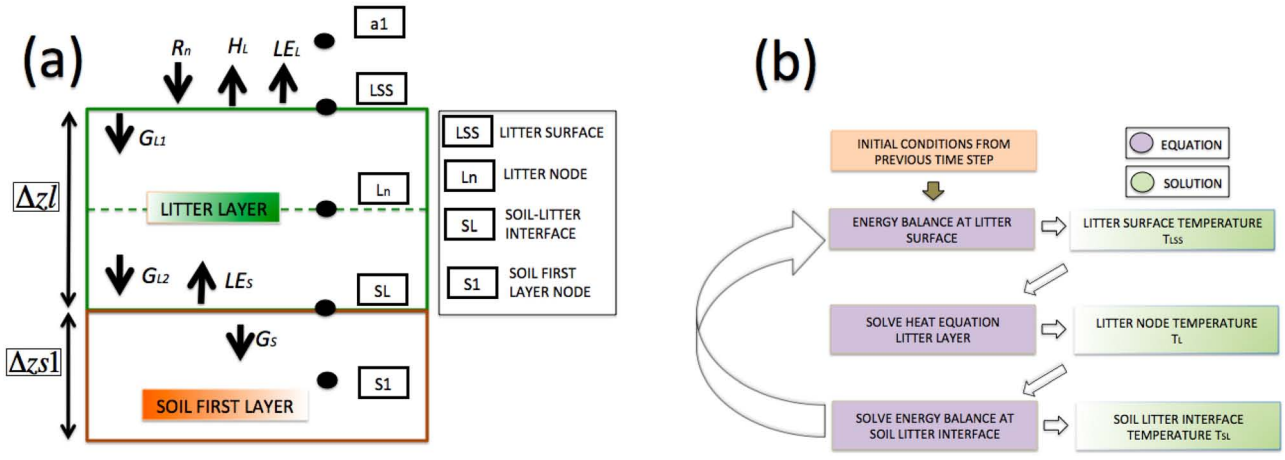

Figure 3. Schematic illustrating the litter model. (a) The litter layer is modeled as a single layer. (b) Iterative Solution flowchart. A numerical implementation is performed to include litter layer dynamics. Energy balance is solved at the litter surface and also at the soil litter interface. Three equations ((1) litter surface energy balance, (2) Litter heat equation, (3) litter-soil interface energy balance) are solved simultaneously using an iterative framework.

present the results from a set of sensitivity analyses designed to disentangle the relative roles of HR, the coupled interactions of different species, and the presence of a litter layer, on the ecohydrological functioning of the land surface. Our focus here is on the surface energy balance and belowground water uptake patterns and resulting soil moisture states. We contrast the situations in which only tall vegetation is present (year 2001) and when both tall and understory vegetation are present (year 2002). We also investigate the role of the hydraulic fuse mechanism, that is, the hydraulic disconnection between roots and soils under extremely dry situations, on the latent heat flux.

4.1.1. Single Species Analysis

[22] For the year 2001, when no understory shrubs are present, Figure 5 shows the daytime (07:00 UTC to 19:00 UTC)

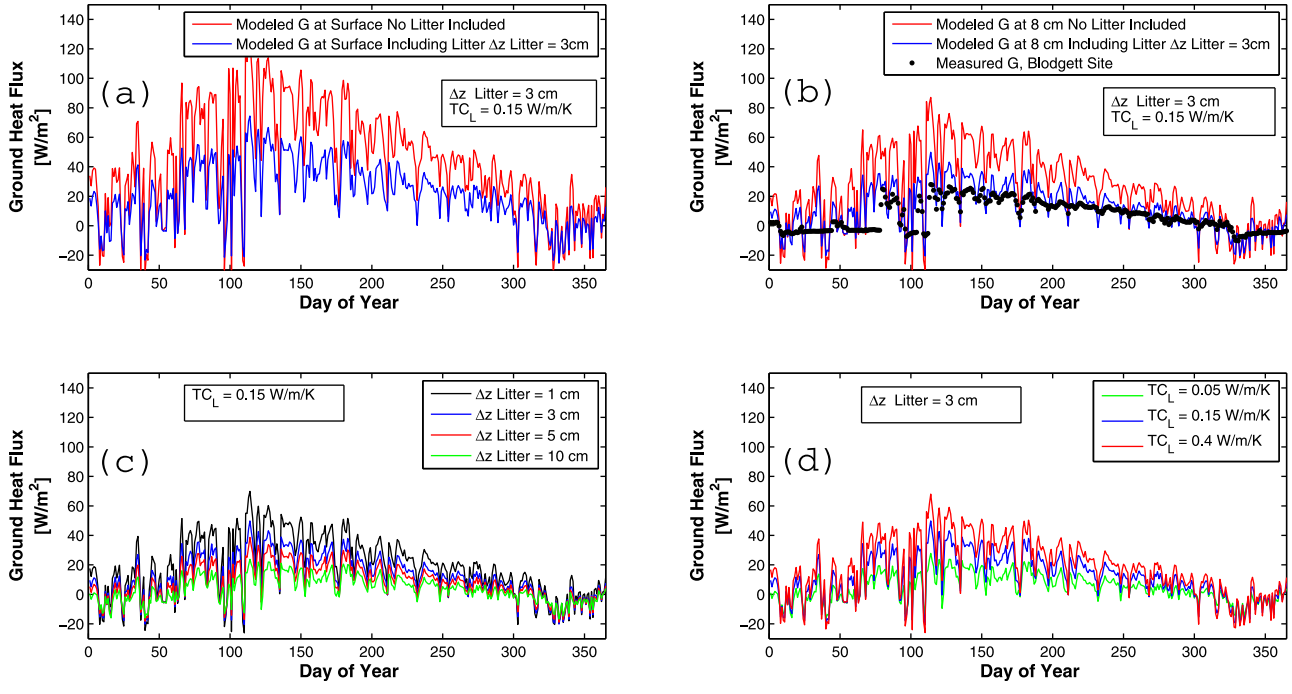

Figure 4. Sensitivity of ground heat flux (G) to litter layer thickness (Δz) and thermal conductivity (TC_L) at the Blodgett site for year 2001. (a) Modeled G at the ground surface with and without litter layer. (b) Measured G at 8 cm below the surface compared with modeled response with and without litter layer. (c) Modeled G at 8 cm below the surface for different litter layer thicknesses, (d) and for different thermal conductivities.

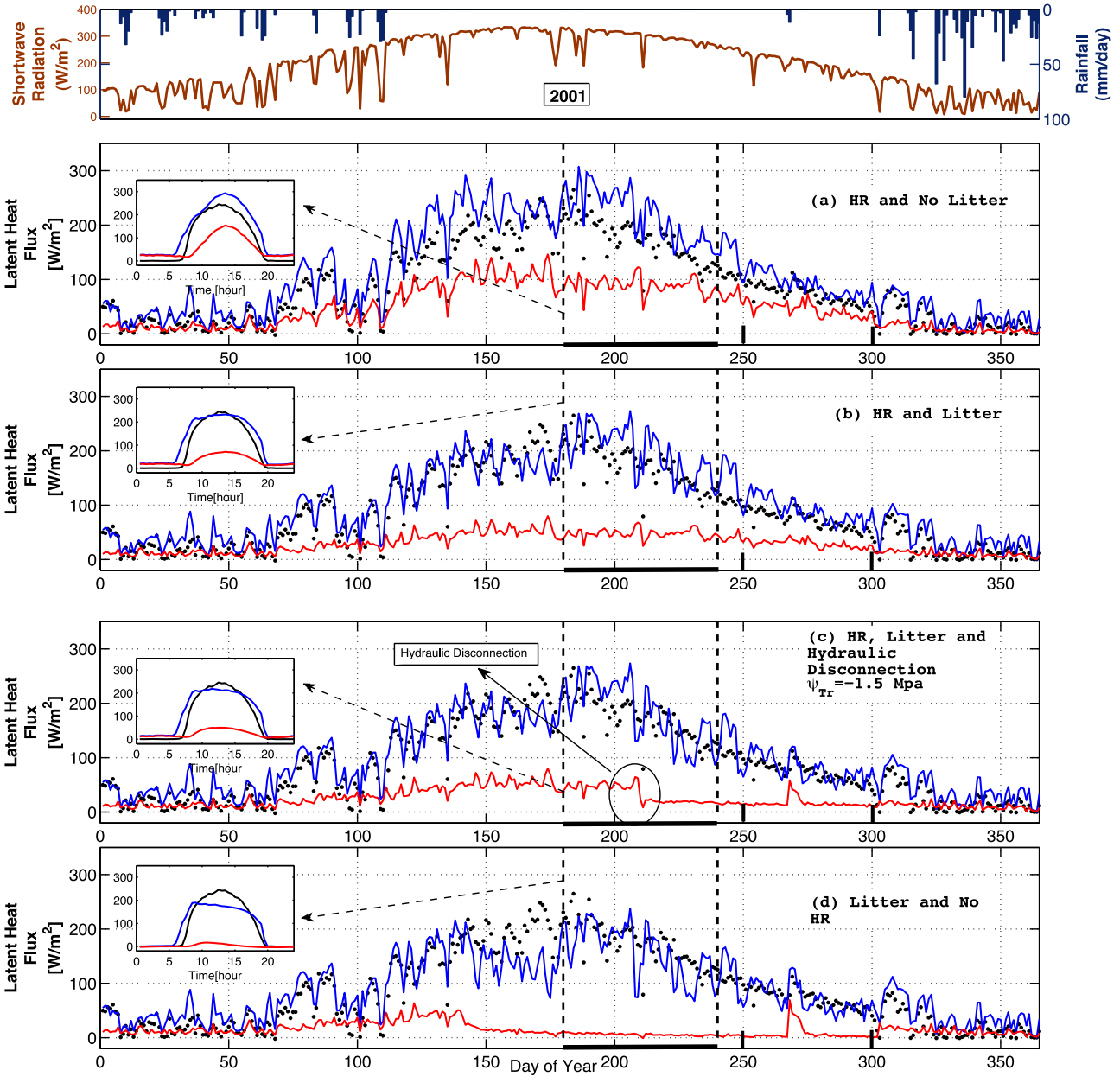

Figure 5. Illustration of the annual variation of the daytime (07:00 UTC to 19:00 UTC) average latent heat flux from ponderosa pine for four different scenarios. (a) HR is included but there is no litter layer above the soil column. (b) HR is included and there is a litter layer above the soil. (c) HR is included, a litter layer lies above the soil column and hydraulic disconnection between the roots and the soil occurs when $\overline{\psi_s} \leq \psi_{Tr}$, where $\overline{\psi_s}$ is the daily average of soil water potential. (d) HR is not included and there is a litter layer above the soil. Blue line indicates the total ecosystem flux consisting of the sum of transpiration and soil evaporation, the red line shows soil evaporation only, and black color indicates observed values. Left insets show the diurnal cycle of the latent heat flux averaged for July and August. For reference the top panel shows the daily average downward shortwave radiation and daily total rainfall for 2001. The coefficient of determination R^2 between simulated and observed latent heat flux for the four cases in Figures 5a–5d are 0.71, 0.81, 0.82 and 0.75, respectively.

average latent heat flux from the ecosystem (LE_{eco}), consisting of contributions from PP (LE_{PP}) and soil evaporation (LE_{soil}):

$$LE_{eco} = LE_{PP} + LE_{soil}. \quad (2)$$

As illustrated in Figure 5, four different cases are examined involving the presence or absence of HR and litter which are compared to observations obtained from the flux tower. Comparing Figures 5a and 5b we see that LE_{soil} is higher when the litter layer is absent. The presence of the litter layer reduces the radiation that reaches the soil underneath,

thereby reducing soil evaporation (Figure 5b). This increases the available soil-moisture for PP, resulting in increased transpiration. The trade-off between transpiration and soil evaporation in these plots demonstrates that PP will make use of available moisture, and that a litter layer suppresses soil evaporation, increasing available water for transpiration.

[23] When HR is switched off (Figure 5d) soil evaporation becomes negligible by the middle of the summer as the shallow layer dries up in early summer and there is no source of moisture replenishment due to the lack of rainfall through the summer. This lack of moisture sources together with the atmospheric demand have been observed to trigger HR [*Warren et al.*, 2007]. Here in the absence of HR we observe that PP transpiration is also reduced during this period. Although the deep roots of PP are able to tap into the deeper reservoirs of moisture in the soil column, the transpiration remains suppressed without HR. As a consequence of the dry near-surface soil layers, most of the energy absorbed by the soil is dissipated in the form of sensible heat flux and longwave radiation emission as the surface warms.

[24] When compared to the observations we see that the absence of litter results in an overestimation of the fluxes of *LE* during the summer period (Figure 5a). When litter is present there is a better agreement with the measurements during the summer period, (Figure 5b), however it still overestimates the fluxes in the late summer and autumn (days 250–300). In the absence of HR the ecosystem *LE* flux is underestimated during most of the summer period (Figure 5d) although there is a better match in the late summer and autumn period. The observations show a pronounced decrease in *LE* in the late summer which seems to be produced by water stress.

[25] As the soil column becomes dry and the soil moisture potential drops, an efflux of water from the root to the soil can occur. To prevent such situations a hydraulic disconnection between the roots and the soil is triggered when the daily average $\overline{\psi_s}$ falls below a threshold ψ_{Tr}. This threshold indicates the onset of the hydraulic disconnection. However, the threshold is species specific [*Espeleta et al.*, 2004] and relies on several physiological variables which are difficult to obtain for a particular site and species. The standard value for the wilting point is $\psi_{Tr} = -1.5$ MPa. Although other studies have adopted different values for the wilting point (e.g., *Rose et al.* [2003] uses $\psi = -2.2$ MPa as a threshold for Jeffrey pine and manzanita shrubs) we use $\psi_{Tr} = -1.5$ MPa in this study. Once the daily average soil matric potential in any layer reaches the wilting point the root radial hydraulic conductivity is set to zero, that is, it is modeled as a threshold mechanism, which prevents both uptake and release of water in the layer. This disconnection remains until the daily average soil matric potential increases again above the threshold.

[26] Figure 5c shows the *LE* fluxes resulting from the simulation in the presence of litter, HR and hydraulic disconnection. Simulations showed that hydraulic disconnection occurs only in the topmost layer. The immediate consequence of this is a significant reduction in soil evaporation. The inclusion of hydraulic disconnection, along with the HR and litter layer dynamics, produce simulated *LE* fluxes that resemble better the observations from Blodgett during the late summer (Figure 5c) and do not show the early shut off of soil evaporation characteristic of the absence of HR (Figure 5d). This leads us to conclude that each of these components has an important role to play in this ecosystem.

4.1.2. Multispecies Analysis

[27] The presence of shrubs in the year 2002 adds an additional complexity to the moisture dynamics. The total ecosystem latent heat flux now includes a contribution from shrubs, LE_{shrubs}, and is given as

$$LE_{eco} = LE_{shrubs} + LE_{PP} + LE_{Soil}. \quad (3)$$

Figure 6 shows the components of LE_{eco} for the same set of sensitivity simulations presented in Figure 5, but for the year 2002 with the inclusion of shrubs. The simulations for 2002 were started from the conditions at the end of the 2001 simulation runs. HR has been observed in different shrub species [*Prieto et al.*, 2010; *Muñoz et al.*, 2008], and so we allow for HR to be present in shrubs for these simulations. In Figures 6a, 6b, and 6c, HR is enabled in both PP and shrubs while in Figure 6d HR is switched off for both PP and shrubs.

[28] Soil evaporation during summer in the presence of shrubs (Figure 6a and 6b) is smaller compared to that without them (Figure 5a and 5b). Shrubs rely more on near surface moisture than PP due to their more shallow root profile, making soil evaporation a process that significantly impacts the energy balance of shrubs. In Figure 6a the summer soil evaporation is higher than in Figure 6b due to the absence of the litter layer. As in Figure 5d, Figure 6d shows that in the absence of HR soil evaporation drops during the middle of the summer because there are no sources of water to replenish the depleted near-surface soil moisture. The total latent heat flux released by the ecosystem is higher in the presence of HR.

[29] Although the rate of transpiration in shrubs is considerably smaller than PP (Figure 6) the strong dry conditions during summer create water stress in the near-surface domain. Since the roots of shrubs are more confined to the near-surface zone of the soil column they are more vulnerable to this drying. HL by PP during the summer plays an important role in supporting both shrub transpiration and soil evaporation. It is interesting to note that in 2002 the presence of shrubs avoids the triggering of hydraulic fuse by reducing the moisture loss due to soil evaporation.

[30] The dynamics observed in Figures 5 and 6 are a strong function of the processes occurring belowground. Figure 7 shows the monthly mean values of root water uptake through the soil column for year 2001 and 2002 for the four scenarios analyzed above. Figure 7a shows that when no litter is included, the evaporative demand from the soil-surface during summer establishes a steep gradient between the soil and root water potential and results in a significant release of moisture from the roots in the near-surface zone, i.e., negative uptake values. This moisture, supplied by moisture taken up from the deeper layers by PP, contributes to high values of LE_{soil}. By comparing the year without shrubs (2001) to that with shrubs (2002), we see that the presence of shrubs results in an increased uptake by PP from the deeper layers, and a reduced release

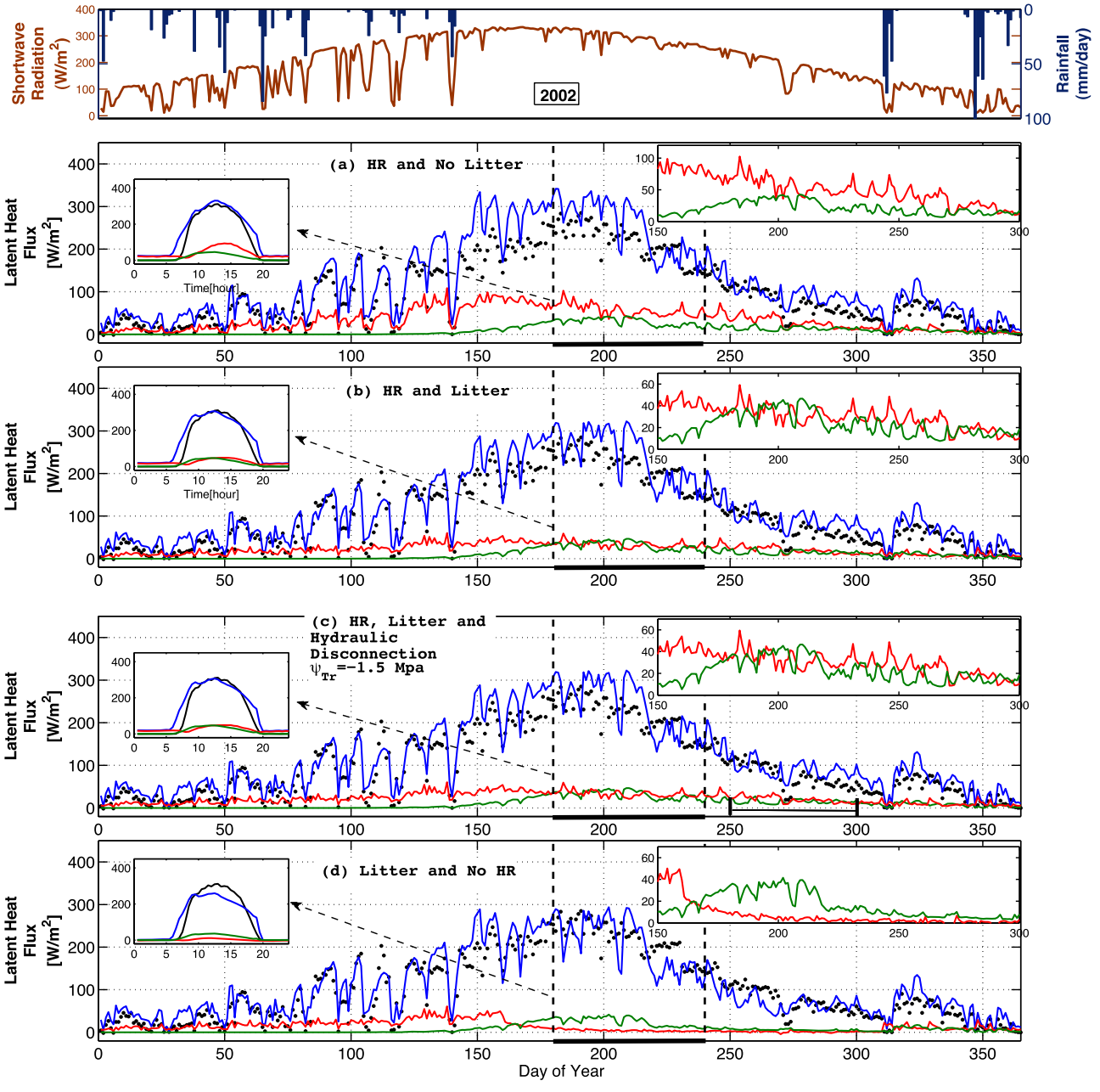

Figure 6. Same as Figure 5 but for the presence of two vegetation species, PP and shrubs, during 2002. Green lines represent the flux from the shrubs and the inset on the right shows the comparative details between the latent heat from soil evaporation (red) and shrub transpiration (green). The coefficient of determination R^2 between simulated and observed latent heat flux for the four cases in Figures 6a–6d are 0.72, 0.80, 0.80 and 0.82, respectively.

in the near surface zone. This is in part due to the increased shading of the ground surface by the shrub cover. We also note the presence of hydraulic descent during the rainy periods. Comparing Figure 7b with 7a we see a similar pattern but the presence of litter reduces soil evaporation and this is reflected in a reduction in the release of moisture from the roots in the near-surface zone. Again we note higher uptake of water by PP and reduced moisture release near the surface in the presence of shrubs.

[31] In Figure 6c hydraulic fuse is not reached and therefore there is a continuous efflux of moisture from the roots to the soil surface during the summer of 2002. The rate of this efflux is smaller in comparison to year 2001 when shrubs were absent. This efflux of water helps to sustain the water potential in the soil surface above the threshold ($\psi_{Tr} = -1.5$ MPa). In the absence of HR shown in Figure 7d, the water uptake shows less complex dynamics where the water uptake during the summer is from the deeper layers but at much reduced levels due to the absence of nighttime transport to dry shallow layers. These results, although qualitatively similar to earlier studies [e.g., *Amenu and Kumar*, 2008], extend our understanding with regards

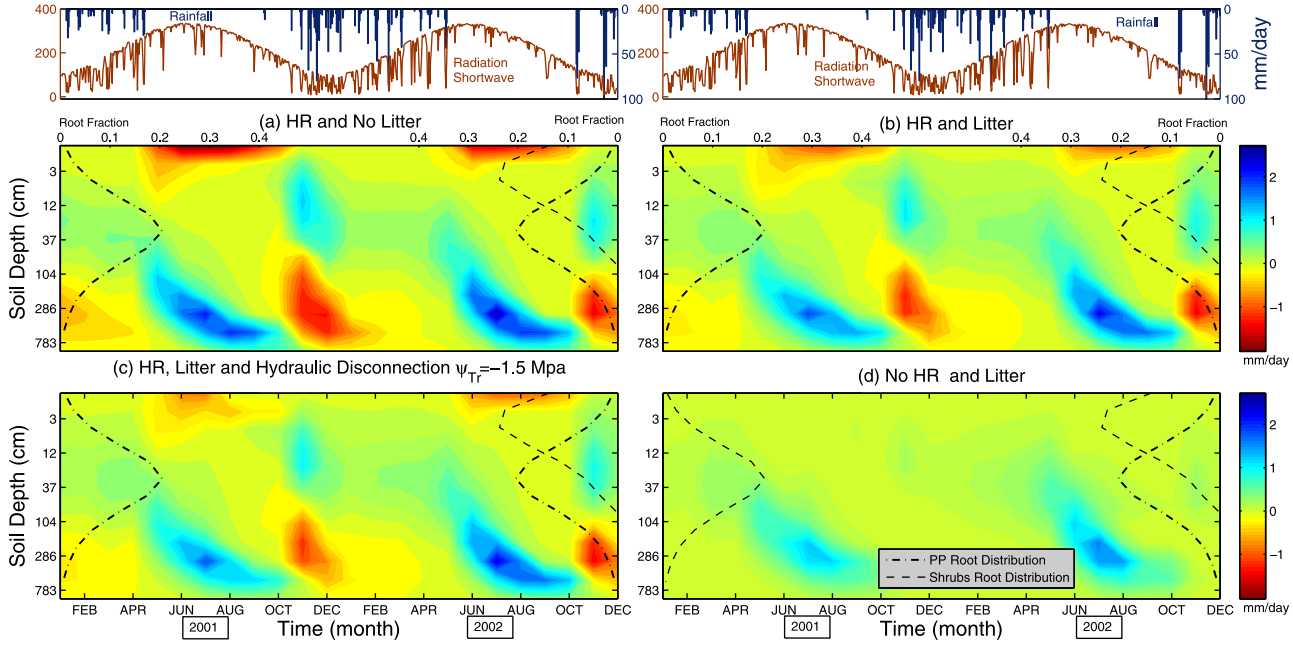

Figure 7. Water uptake patterns by vegetation in 2001 and 2002 corresponding to the four scenarios presented in Figures 5 and 6 (negative values imply moisture release from the vegetation roots to the soil). The dashed and dot-dashed lines overlaid on the color panel indicate the root distribution for shrubs and PP, respectively. (a) HR is included but there is no litter layer above the soil column. (b) HR is included and there is a litter layer above the soil. (c) HR is not included, a litter layer lies above the soil column and hydraulic disconnection between the roots and the soil occurs when $\overline{\psi_s} \leq \psi_{Tr}$, where $\overline{\psi_s}$ is the daily average of soil water potential. (d) HR is not included and there is a litter layer above the soil. For reference the top panel shows the daily average of downward shortwave radiation and daily total rainfall for 2001 and 2002.

to the role of shrubs, soil evaporation and a litter layer in the HR dynamics.

4.2. Summer Season Diurnal Dynamics

[32] The results presented above have revealed interesting patterns of seasonal dynamics based on the analysis of daily average values. In this section we analyze the interaction between different vegetation species and moisture transport at the diurnal time scale using the half-hour observed and simulation data. We analyze the same four scenarios as illustrated in Figures 5, 6 and 7.

[33] Figure 8 (top) shows the mean diurnal water uptake dynamics by PP in 2001, when shrubs are not present. In Figures 8a and 8b there is a continuous redistribution of water to the top layer throughout the day by PP, indicated by negative uptake values. The top layer is the thinnest layer in the numerical simulation (1.7 cm of thickness) and is in direct contact with the atmosphere unless a litter layer is present. The radiative energy reaching the surface in summer creates a high evaporative demand for moisture. Apart from moisture due to HL and dew in the night, there is no other source of moisture replenishing the surface layer. As a consequence, $\psi_s \leq \psi_r$ for the top layer throughout the day. Note that the moisture released by the roots is highest in the afternoon. There is HL in the night also, albeit at lower volumes, that moves the water to the near surface layer which in turn supports the evaporative demand during the day. Some experimental studies have reported daytime redistribution [*Burgess et al.*, 2000; *Scholz et al.*, 2002; *Espeleta et al.*, 2004]. HR is enhanced by the low water potential that arises in shallow soil layers during dry periods. The importance of HR in regulating soil moisture in this critical zone during prolonged droughts has been indicated in recent studies [*Warren et al.*, 2011].

[34] When litter is considered in the simulation (Figure 8b), the flux of water redistributed to the top layer is reduced considerably but not eliminated. Figure 8c shows the dynamics in water uptake when hydraulic disconnection is also enabled. Although the average shown in Figure 8c for July and August includes several days before the hydraulic disconnection is triggered, we see that the efflux of water in the top layer is reduced.

[35] In Figure 8, the middle and bottom rows show the diurnal average water uptake by PP and shrubs, respectively, in 2002 when both species are present. Shrubs uptake water from the shallow (up to 100 cm depth) soil layers. Thus the presence of shrubs generates a new demand that competes with soil evaporation for hydraulically lifted water. The water uptake patterns by PP are different in 2002 as compared to 2001. In 2002, under the presence of shrubs, the water released by PP to the surface is reduced. Instead PP release increases in deeper layers located between 6 and 80 cm where the transpiration use by the shrubs creates a water potential gradient that results in efflux of water out of the pine roots.

[36] In the shallow soil layers both PP and shrub roots are present and compete for water uptake during the

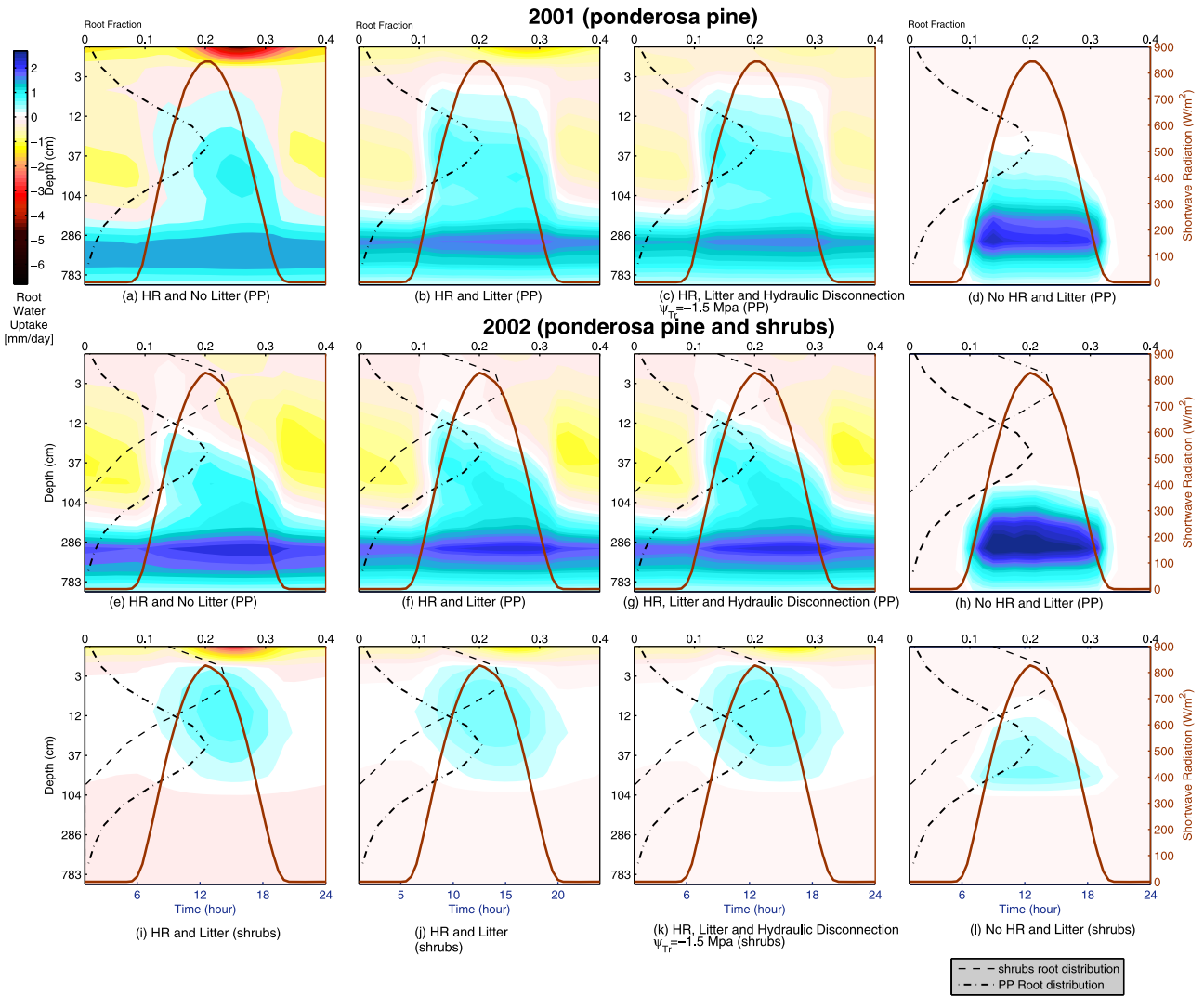

Figure 8. Diurnal pattern of water uptake by PP and shrubs in summer (July–August) for the four scenarios discussed in Figures 5 and 6. (a, e, i) HR is included but there is no litter layer above the soil column. (b, f, j) HR is included and there is a litter layer above the soil. (c, g, k) HR is not included, a litter layer lies above the soil column and hydraulic disconnection between the roots and the soil occurs when $\overline{\psi_s} \leq \psi_{Tr}$, where $\overline{\psi_s}$ is the daily average of soil water potential. (d, h, l) HR is not included and there is a litter layer above the soil. First row shows the water uptake in 2001 by PP. Second row and third row shows water uptake by PP and shrubs, respectively, during 2002 when the two species are present. The presence of litter and shrubs influences the dynamics of water uptake in the soil. Redistribution of water to the soil surface occurs during the daytime also due to the gradient created from the high evaporative demand. The presence of litter and shrubs decreases the efflux of water observed at the surface.

daytime. The competition for water is dictated by equation (1) and the capacity of each plant species to uptake water at a given layer is determined by the root radial conductivity, which in turn is a function of the root distribution and fine root biomass [*Amenu and Kumar*, 2008]. In the shallow layers shrubs have higher root radial hydraulic conductivity and, therefore, are more efficient in the uptake of water. The deeper distribution of root biomass makes PP more efficient in water uptake from the deeper layers. The patterns of water uptake and release by shrubs are less prominent than the ones by PP as the redistribution of water by HR in shrubs is found to be small in comparison with those by PP. As seen already, the presence of litter reduces the near-surface evaporative demand. Figure 8g also shows the uptake pattern when the hydraulic disconnection mechanism is implemented, but as mentioned before hydraulic fuse is not triggered in this case, suggesting that the presence of shrubs reduces near-surface drying that would occur for PP alone. Note that under No HR scenario (Figure 8h) the water uptake patterns are not significantly different from that of the single species case. The third row in Figure 8 shows the water uptake pattern for shrubs. We see that, as expected, most uptake is supported in the middle layers where the release by PP during the night provides the moisture to support the transpiration demand of shrubs during the day.

[37] Figures 9a, 9c, and 9d show observed data of soil moisture from a single point measurement and model results for year 2002 at three different depths (10, 30, and 50 cm). The model with both HR and No HR capture the general trend quite well. We should not expect an exact match between modeled and observed soil moisture since observations are at a specific point under the vegetation whereas the model represents the spatial average behavior. Figure 9b shows the soil moisture dynamics at 10 cm between days 150 to 166 which are located at the beginning of the summer with no rainfall occurring during this period. In this figure the diurnal cycle of soil moisture can be observed in more detail showing the oscillating pattern which is characteristic of HR. Note that the No HR simulations does not show this behavior. The inset figure shows the diurnal cycle of soil moisture averaged between days 150 to 166 for the observed and the model result in the presence of HR. In both cases it can be seen that there is an increase of soil moisture during the night due to efflux from roots and a reduction during the day due to transpiration.

4.3. Competitive and Mutualistic Dependencies

[38] The above results suggest that the dynamics of the multispecies composition at the Blodgett site are best represented through considerations of HR and litter dynamics along with the hydraulic disconnection mechanism. The set of sensitivity simulations that selectively incorporate different subsets of these functions have helped us understand the significance of each component on the latent heat flux and belowground water uptake, release, and transport patterns. Figure 10 sheds more light on the trade-off between the different components of water use. When there is No HR, LE_{soil} is small and LE_{shrubs} can reach over 40 W m^{-2} (triangles in the Figure 10a). Note that the color of the symbols in Figure 10a are associated with the total vegetation LE while the size of the symbols are associated with LE_{PP}. The transpiration for PP and shrubs is supported by soil moisture uptake from the middle and deeper layers (Figure 8, fourth column). Together they increase the LE_{eco} (darker green color). However, when HR is considered (squares and stars in Figure 10a), both LE_{soil} and LE_{shrubs} are higher and there is a trade-off between them as characterized by the dotted line obtained from the regression on the largest 10% of the values. That is, LE_{shrubs} increases as LE_{soil} decreases. However, it is noteworthy that the high values of LE_{shrubs} are larger than the case when there is No HR. We also note that LE_{PP} increases (larger boxes and stars) as LE_{shrubs} increases and LE_{eco} is higher (darker green color) as a result. This is a result of higher uptake of water by PP and shrubs (Figure 8, column 1 and 2). When we compare the presence (boxes) and absence (stars) of litter in Figure 10a, we see that by reducing the energy reaching the soil surface, the litter has the net effect of increasing LE_{shrubs}. Also the presence of litter enhances the fluxes LE_{PP} and productivity for PP. These are further exemplified in Figures 10b and 10c where the presence of litter results in higher latent heat as captured by the points which trend upward of the 1:1 line. This analysis establishes that the trade-off in water use occurs in a way that benefits both the tall and understory vegetation and facilitates increase in

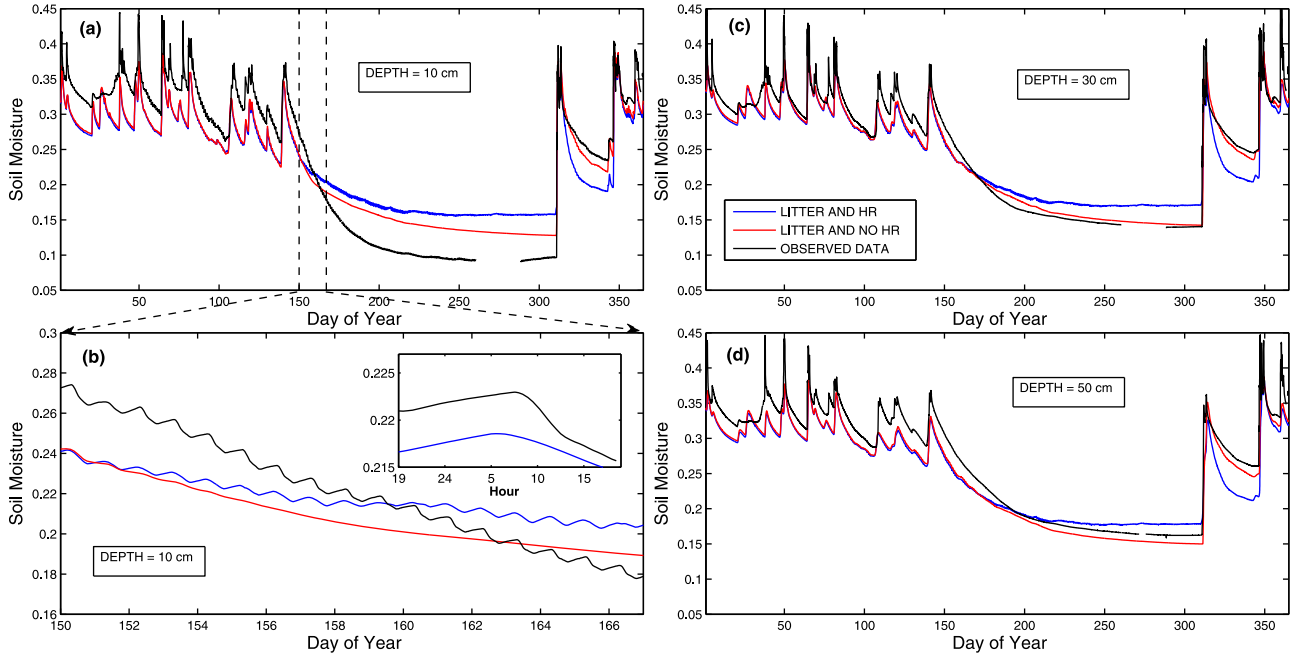

Figure 9. Soil moisture dynamics at the Blodgett site during the year 2002 at depths of (a) 10 cm, (c) 30 cm and (d) 50 cm. Observed data is compared with the model simulation in the presence and absence of HR. (b) Soil moisture at 10 cm is shown in more detail for days 150 to 166 which correspond to the beginning of the dry summer period. The inset figure shows the diurnal cycle of the observed and modeled (HR presents) soil moisture averaged over days 150 to 166. Since No HR simulations do not show an increase in nighttime soil moisture, they are not plotted in the inset figure.

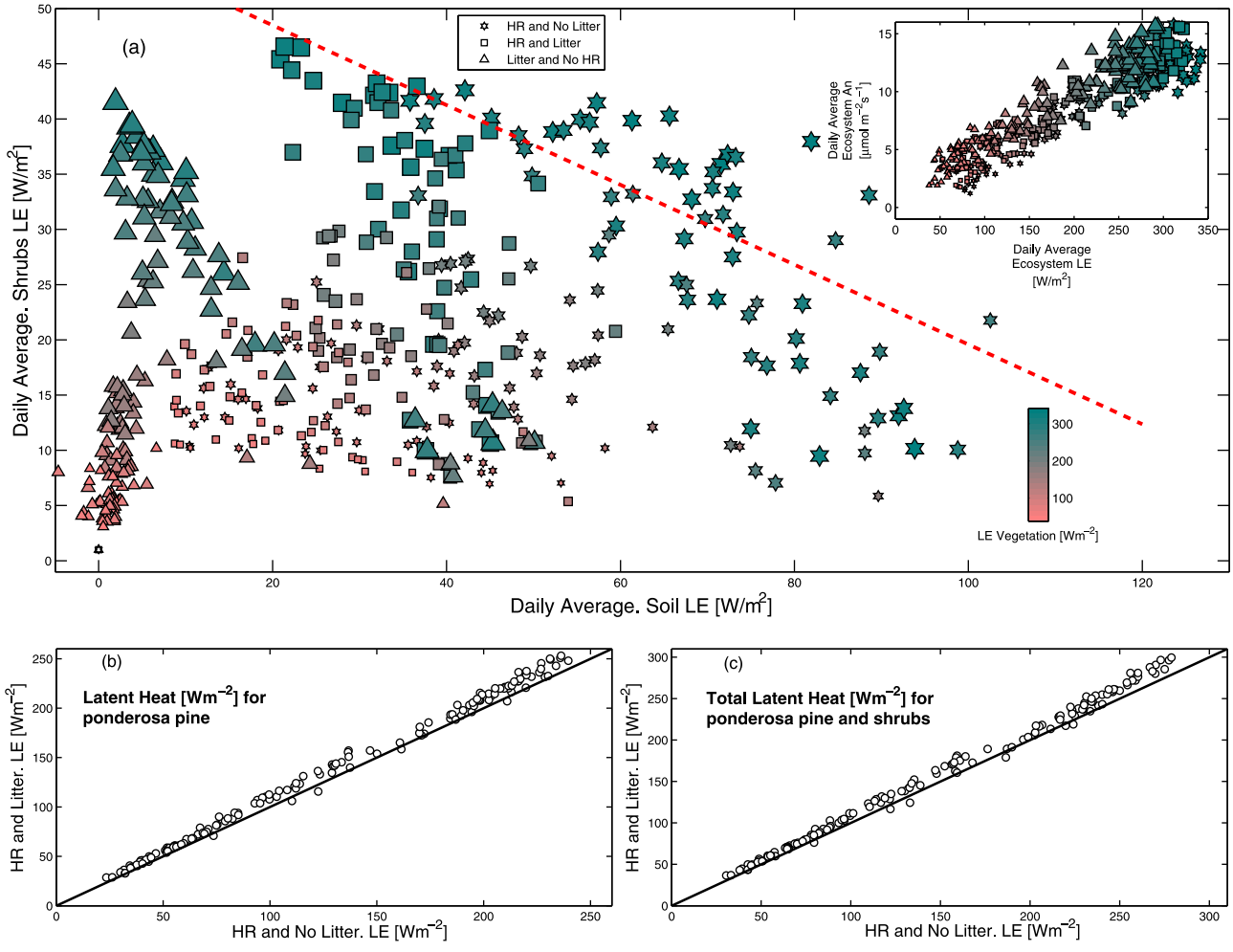

Figure 10. (a) Illustration of the trade-off between soil evaporation and shrub transpiration. This trade-off is influenced by the presence of HR and litter. In the absence of HR, soil evaporation fluxes are small (triangles). When HR is enabled, the presence of litter damps the radiative energy reaching the soil (compare stars and boxes), thereby reducing the soil evaporative demand and therefore reducing the efflux of water from the roots to the near-surface soil. This enhances shrub transpiration. Larger symbols indicate higher latent heat from ponderosa pine, and greener color indicates higher total vegetation latent heat flux. The dotted red line is the regression line for the highest 10% of the values showing the trade-off. The inset figure shows the relationship between daytime average transpiration and photosynthetic CO_2 assimilation. (b) Scatterplot of LE release by the ponderosa pine in the presence and absence of litter. (c) Scatterplot of LE release by the ponderosa pine and shrubs in the presence and absence of litter.

total ecosystem productivity. The role of litter layer in nutrient cycling and its impact on ecosystem productivity is presently being studied.

[39] Figure 11a shows the total net carbon assimilation A_n from the model and that reconstructed from Blodgett observations for 2002. Comparison of model predictions in the presence and absence of HR (see Figures 11b, 11c, and 11d) capture the expected higher productivity of shrubs in the presence of HR. However, the dependence of shrubs on water redistributed by PP trees is regulated by their root depth and therefore their capacity to reach deeper layers. Due to the uncertainties in maximum shrub root depth during 2002 three different maximum shrub root depths, ranging from 60 to 140 cm, were analyzed (Figures 11b, 11c, and 11d). For the 85 cm depth, the presence of HR results in an additional C uptake of 2 mol m^{-2} in 2002 which comprises 28% of the net C uptake by the shrubs in that year. For the case of 140 cm depth, the presence of HR results in an additional C uptake of 0.9 mol m^{-2} in 2002 which comprises 13% of the net C uptake by the shrubs in that year. As expected, the difference in net shrub productivity between HR and No HR is reduced as the shrub root system becomes deeper. Although the differences in shrub C uptake in the presence or absence of HR is small compared to the PP net uptake (~45 mol m^{-2}), these numbers comprise an important fraction of the shrub budget at this stage.

5. Summary and Discussion

[40] In this study we analyzed the roles of three potentially important ecohydrological processes and their interactive

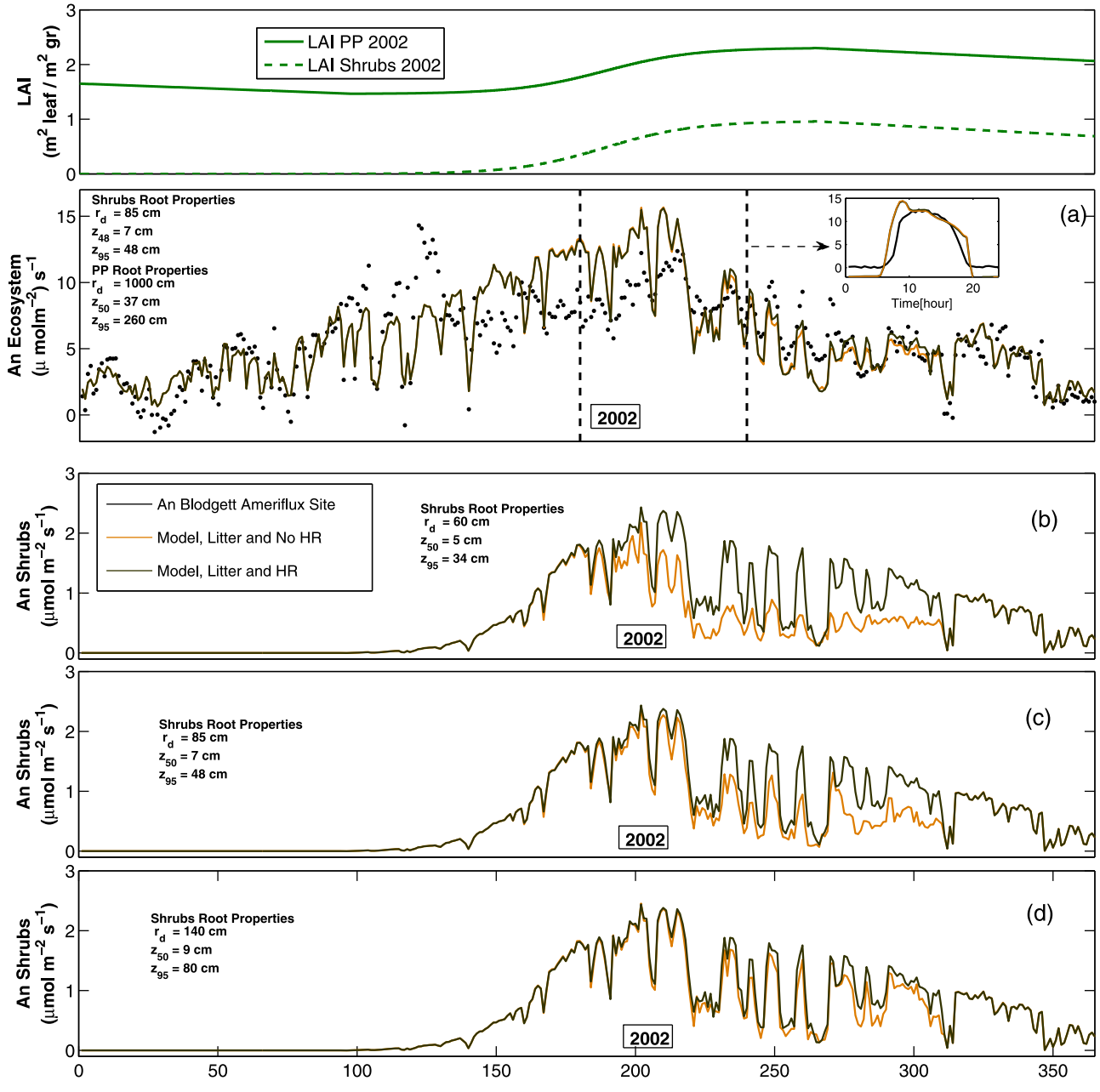

Figure 11. Illustration of the annual variation of daytime (07:00 UTC to 19:00 UTC) carbon assimilation in the presence and absence of HR in 2002. (a) Net carbon assimilation by the ecosystem. Net carbon assimilation by shrubs with maximum root depth equal to (b) 60 cm, (c) 85 cm, and (d) 140 cm. The presence of HR enhances the net carbon assimilated by shrubs. Top panel shows the *LAI* of ponderosa pine and shrubs.

effects. The three processes were hydraulic redistribution, the modulation of soil fluxes by a litter layer, and hydraulic disconnection in the context of a single and multispecies vegetation composition. Our goal was to disentangle the role of each of these processes in root water uptake and vertical soil moisture distribution through a resolved soil column, providing insight into the impacts on land-atmosphere energy partitioning and carbon dioxide exchange. The Ameriflux site at the Blodget Forest in the Sierra Nevada region of California provided an ideal setting to examine the impacts of these ecohydrologic processes in a multispecies system forced by a Mediterranean climate, in which water plays a dominant role in controlling ecosystem function.

[41] Previous studies have indicated the potential for HR to enhance soil evaporation [*Caldwell et al.*, 1998], and numerical studies have shown the impact of HR in soil evaporation [*Lee et al.*, 2005; *Wang*, 2011]. These studies turn off HR in the near-surface layer during dry periods. Although there is experimental evidence that fine roots die at low soil water potentials and the response to drought is species and site specific [*Espeleta et al.*, 2004], the interaction between different variables such as wilting point, the

presence or absence of litter, hydraulic redistribution, and soil evaporation regulate the redistribution of water to the surface which is a critical process that merits further study. To our knowledge these interactions between the hydraulic redistribution of moisture through the soil system by roots, and soil evaporation (see Figures 5 and 6) have not been analyzed and quantified in experimental or numerical studies. Our results show that as the summer progresses, the available moisture at the soil surface decreases such that the soil potential in near-surface layers drops below the water potential of the coincident roots. This potential gradient drives the uplift of moisture from moister lower layers to the shallow soil layers through HL (Figures 7 and 8). This upward transport of moisture is nearly continuous in time during extensive dry periods (Figure 8). Simulations conducted without HR show a reduction in soil evaporation during these periods, indicating that HR supplies moisture to near surface layers, which is then evaporated, effectively resulting in an enhanced loss of moisture from the system. Previous simulations have focused mainly on transpiration and have neglected soil evaporation [*Amenu and Kumar*, 2008; *Mendel et al.*, 2002]. When soil evaporation was not considered (results not shown) the results obtained by our simulations resembled the general dynamics of water uptake reported previously [*Amenu and Kumar*, 2008].

[42] In natural ecosystems, the presence of a litter layer affects energy and mass balance at the surface [*Park et al.*, 1998; *Ogee and Brunet*, 2002] with impacts on soil evaporation. Here we introduced a litter layer above the soil column in the numerical model to analyze these dynamics. The inclusion of a litter layer reduces the radiation flux reaching the soil surface, thus reducing the soil evaporative demand. This reduces the potential gradient between the soil and the roots which in turn decreases the efflux of moisture from the roots to the soil (Figures 5 and 6). Despite the reduction in soil evaporation due to the existence of a litter layer, HR moves moisture from deeper soil layers to shallow soil layers throughout the summer months (Figure 7). It has been argued that this enhances fine root longevity [*Pregitzer et al.*, 1993; *Caldwell et al.*, 1998] in those layers, resulting in enhanced moisture uptake once precipitation recommences. It is also possible that higher moisture levels support decomposition of organic matter [*Caldwell and Richards*, 1989; *Caldwell et al.*, 1998; *Horton and Hart*, 1998; *Dawson*, 1993]) as well as facilitating nutrient mass transport and the diffusion of ions in the soil [*Nye and Tinker*, 1977; *Caldwell and Manwaring*, 1994].

[43] Under moisture stress plants seek to meet the transpirational water demand while avoiding critical negative water potentials that may cause cavitation [*Alder et al.*, 1996; *Tiree and Sperry*, 1988]. When shrubs are present, the trigger for hydraulic fuse is dependent upon the depth of the shrubs roots. Shallower shrubs roots prevent hydraulic disconnection as shown in our results, but sensitivity studies showed that as the root density of shrubs go deeper, the hydraulic fuse is triggered resulting in disconnection. *Domec et al.* [2004] found that the presence of HR in two different tree species (ponderosa pine and Douglas fir) helps to mitigate embolism because it sustains higher levels of soil water potential in shallow layers (20–30 cm). However, under extreme stress, plants may develop specific strategies to reduce the hydraulic connection with the soil [*Caldwell et al.*, 1998; *Espeleta et al.*, 2004], for example, death of fine roots [*Espeleta et al.*, 2004]. To explore the role of such strategies, we incorporated hydraulic fuse as a threshold mechanism. When the hydraulic fuse is triggered there is a sharp reduction in the latent heat flux during the middle of the summer and captures the signature of the observed fluxes during this period when shrubs are not present. These results demonstrate that the stomatal control on transpiration, or even standard approaches to modeling root moisture uptake, may not be sufficient to accurately predict water fluxes in protracted dry situations.

[44] Figures 5, 6, 7, and 8 show only one scenario of hydraulic disconnection that corresponds to a threshold $\psi_{Tr} = -1.5$ MPa corresponding to a standard value for wilting point. As mentioned in section 4, it is challenging to estimate a specific value of wilting point for a particular place and species. When the threshold was established as $\psi_{Tr} = -2.2$ MPa (adopted in the work of *Rose et al.* [2003]) hydraulic fuse does not occur if litter and HR are present. However this threshold is exceeded if litter is absent. In the absence of litter and presence of HR the daily average of soil water potential reaches $\overline{\psi_s} = -3.8$ MPa. Although there is an uncertainty regarding the wilting point at the surface, the presence of litter has a significant impact on the soil water potential on the surface, and therefore in triggering hydraulic fuse. We believe that these results may have important implications for drought studies where extended dry periods may have implication for root longevity, water uptake, and ecosystem resilience.

[45] Natural ecosystems are characterized by the coexistence of multiple vegetation species which have different aboveground and belowground structural and ecophysiological characteristics. Several studies have pointed to the importance of HR in multispecies ecosystems [*Dawson*, 1993; *Emerman and Dawson*, 1996; *Moreira et al.*, 2003; *Espeleta et al.*, 2004; *Brooks et al.*, 2006]. The inclusion of shrubs in the model modified the water uptake dynamics (Figure 8), by altering the water potential gradient in the vicinity of the shrub roots, resulting in more water being redistributed to layers below the surface that contain the roots of the shrubs while reducing that in the surface layer. The deeper root system of PP moves water upward to shallower soil layers where it is utilized to satisfy the transpiration demand of the shrubs throughout the summer (Figure 6). The shrubs in turn reduce the soil evaporative demand during the day.

[46] Several previous studies have detected the presence of hydraulically redistributed water by trees with deeper root systems in understory plants [*Dawson*, 1993; *Emerman and Dawson*, 1996; *Brooks et al.*, 2002; *Moreira et al.*, 2003; *Espeleta et al.*, 2004; *Brooks et al.*, 2006]. *Dawson* [1993] found that HR by overstory trees plays an important role in the water dynamics of understory shrubs influencing their growth which is an indirect indicator of productivity. Similarly, *Zou et al.* [2005] found that in some situations HR facilitates shrub performance in a subtropical savanna composed of tree-shrubs communities. On the other hand *Ludwig et al.* [2004] found that competition between plants reduces the facilitative effects of HR. Also *Meinzer et al.* [2004] claimed that the extent to which HR benefits understory shrubs is regulated by the water

potential differences in the soil which is the mechanism that triggers HR. They indicate that this mechanism may start at some point where water requirements have been reduced. Furthermore, *Emerman and Dawson* [1996] found labeled water from HR in understory species but the amount was relatively small which suggests that it is unlikely that this source is causing an effect on shrub performance. The impact of hydraulically redistributed water from overstory trees in understory vegetation is a complex phenomenon that may vary from place to place. The model implemented here is a useful tool to analyze these interactions between different vegetation types. The simulation results obtained in Blodgett suggest that HR is an important mechanism facilitating shrub productivity throughout the long and dry summer. However, the extent to which this mechanism impacts shrub productivity is regulated by shrub root depth. The impact of HR in understory vegetation is stronger as the understory root system is closer to the surface.

[47] The results presented here are based on a numerical model designed to resolve a broad range of physical and ecological functioning through the canopy-root-soil continuum [*Drewry et al.*, 2010a; *Amenu and Kumar*, 2008] in the spirit of exploring novel relationships [*Kumar*, 2011]. The simulations are based on the assumption of passive control on the flow of moisture between the roots and soil driven only by potential gradients. In augmenting the MLCan model with a litter layer and implementing the hydraulic disconnection phenomena, as well as allowing for multiple species interactions, we have been able to confirm that each of these processes plays an important role, at least under specific climatic conditions, in the ecohydrological functioning of a mixed-species Mediterranean system. This study has likewise presented an attempt to represent multiple, interacting species in a detailed ecohydrological model that represents the process of hydraulic redistribution. Our analysis has demonstrated both competitive and mutualistic interactions between the two simulated species, and opens the door to future studies that will further examine the hydrology and biogeochemistry of mixed species systems.

Appendix A: Aboveground *LAD* for Different Species

[48] The leaf area density (*LAD*) representing the vertical distribution of leaves in a canopy of species *i* with height *H* is given by

$$LAD_i(z) = \nu_i(z) LAI_i, \tag{A1}$$

where $\nu_i(z)$ is the distribution function $\left(\int_0^H \nu_i(z)\,dz = 1\right)$, LAI_i is the total leaf area index and $LAD_i(z)$ is the leaf area index of the *i*th plant species. For all species $\nu_i(z)$ is assumed to follow a Weibull distribution with species-dependent parameters α and β. The cumulative distribution function is given as [*Coops et al.*, 2007]:

$$F(z;\alpha,\beta) = 1 - \exp\left(-\frac{1 - z/H}{\alpha}\right)^{\beta}. \tag{A2}$$

By considering *N* vertical layers, the *LAD* for the *i*th species in the *j*th layer can be obtained as

$$LAD_{i,j} = \int_{z_i}^{z_{j+1}} LAD_i(z)\,dz. \tag{A3}$$

Therefore, the fraction from the total leaf area index that belong to a given species *i* at a given layer *j* is given by

$$f_{i,j} = \frac{LAD_{i,j}}{\sum_{i=1}^{M} LAD_{i,j}}. \tag{A4}$$

Appendix B: Litter Model

[49] The litter model uses the framework introduced in previous studies [*Bavel and Hillel*, 1976; *Chung and Horton*, 1987; *Park et al.*, 1998; *Ogee and Brunet*, 2002; *Haverd and Cuntz*, 2010]. The following three coupled equations are solve iteratively until convergence is reached (see Figure 3a for the algorithm and the notation section for a description of the symbols):

B1. Energy Balance at the Litter Surface

[50] At the litter surface

$$R_n \equiv R_{abs} - LW_s = LE_L + H_L + G_{L1}, \tag{B1}$$

where R_n is the net radiation equal to the total radiation absorbed by the soil (R_{abs}) minus the longwave radiation emitted by the soil (LW_s). LE_L is the total latent heat released by the litter and is obtained as

$$LE_L = L_v \rho_d \left[\frac{RH_{Ln} q^*_{Ln} - q_{a1}}{r_a + r_s}\right], \tag{B2}$$

where r_a and r_L are the aerodynamic resistance and the resistance of litter to vapor transport. These resistances are computed using the methodology developed by *Ogee and Brunet* [2002]; *Schaap et al.* [1997]. The sensible heat flux (H_L) is obtained as

$$H_L = \rho_d C_p \left[\frac{T_{LSS} - T_{a1}}{r_a}\right]. \tag{B3}$$

The ground heat flux into the litter (G_{L1}) is obtained as

$$G_{L1} = TC_L \left[\frac{T_{LSS} - T_{Ln}}{\Delta z_L/2}\right]. \tag{B4}$$

Equation (B1) is solved using a numerical root finding function for the temperature at the litter surface (T_{LSS}).

B2. Conservation of Energy Inside the Litter Layer

[51] Assuming that the thermal conductivity remains constant through the litter layer, the heat equation for the litter layer is given by:

$$\frac{\partial T_L}{\partial t} = \alpha_L \frac{\partial}{\partial z}\left(\frac{\partial T_L}{\partial z}\right) \equiv -\frac{\partial G_L}{\partial z}. \tag{B5}$$

The terms T_L, G_L, and α_L in equation (B5) are the litter temperature, heat flux inside the litter layer and litter thermal diffusivity. We implement a simple numerical solution of the heat equation using an implicit scheme and just one layer to get

$$T_{Ln}^{j+1} = \frac{(4\eta(T_{LSS}^{j+1} + T_{SL}^{j+1}) + T_{Ln}^{j})}{(1+8\eta)}, \tag{B6}$$

where

$$\eta = \frac{\alpha_L \Delta t}{\Delta z_L^2}. \tag{B7}$$

B3. Energy Balance at the Soil-Litter Interface

[52] The ground heat flux from the litter layer to the soil (G_{L2}) is given as

$$G_{L2} = LE_s + G_s, \tag{B8}$$

where

$$G_{L2} = TC_L\left[\frac{T_{Ln} - T_{SL}}{\Delta z_L/2}\right]. \tag{B9}$$

The latent heat emitted from the soil (LE_s) is obtained as

$$LE_s = L_v \rho_d \left[\frac{RH_{S1} q_{S1}^* - q_a}{r_a}\right]. \tag{B10}$$

The ground heat flux into the soil (G_s) is obtained as

$$G_s = TC_{s1}\left[\frac{T_{SL} - T_{S1}}{\Delta z_{s1}/2}\right]. \tag{B11}$$

The relative humidity in the topsoil layer is computed as

$$RH = \exp\left[\frac{-g\psi}{R_w T}\right], \tag{B12}$$

where R_w is the gas constant for water vapor and ψ is the water potential. In the case of the litter the water potential is computed as [*Ogee and Brunet*, 2002]

$$\psi_L = \psi_{LL}\left[\frac{\rho_w \theta_L}{\rho_b}\right], \tag{B13}$$

where θ_L is the soil water content in the litter layer. The dynamics of water in the litter layer are calculated based on simple mass balance.

Appendix C: Stomatal Conductance

[53] Stomatal conductance g_s is obtained using the Ball-Berry model [*Ball and Berry*, 1982] that is coupled to the soil-moisture state using the approach of *Tuzet et al.* [2003]. This modified model is given as

$$g_s = f_{sv} \cdot m \cdot \frac{A_n \cdot h_{LS}}{C_{LS}} + b, \tag{C1}$$

where intercept b and the slope m are regression parameters, A_n is the net uptake of CO_2 through photosynthesis, h_{LS} is the relative humidity at the leaf surface and C_{LS} is the CO_2 concentration at the leaf surface. The moisture-dependent parameter [*Tuzet et al.*, 2003] $f_{sv}(\psi_l)$ varies between 0 and 1, and is given as

$$f_{sv}(\psi_l) = \frac{1 + \exp[s_f \cdot \psi_f]}{1 + \exp[s_f(\psi_f - \psi_l)]}, \tag{C2}$$

where s_f is a sensitive parameter, ψ_f is a reference water potential value and ψ_l is the leaf water potential.

[54] The implementation of this Tuzet-Ball-Berry model requires four different species-specific parameters (m, b, ψ_f, s_f). The quantification of these parameters is usually obtained from intensive experimental studies involving different measurements, both belowground and aboveground. Here, we use experimental information reported for the Blodgett Ameriflux site by *Misson et al.* [2004] who analyzed information taken in PP trees [*Panek*, 2004]. They obtained values of $f_{sv}m$ and b and analyzed the trend of these parameters under different conditions of ψ_l. Here we use $m = 13$ which is in the range of values found by *Misson et al.* [2004]. Parameter b varies in the range 0–1.3 mol m^{-2} s^{-1}. Due to the high uncertainty produced by this range of values we computed g_s using information from the Ameriflux tower in year 2000 during wet periods (winter) where LE is similar in the presence or absence of HR. Values of stomatal conductance for shrubs were not available for the site and they were set to the same value as that of PP (Table 1).

Notation

A_n	net uptake of CO_2 through photosynthesis
C_p	specific heat of air
C_{LS} Co_2	concentration at the leaf surface
b	Ball-Berry intercept
f_{sv}	Tuzet-Ball-Berry parameter for the stomatal conductance
G_{L1}	ground heat flux into the litter layer
G_{L2}	ground heat flux from the litter layer into the soil-litter interface
G_s	ground heat flux into the soil
g	acceleration due to gravity
g_s	stomatal conductance
h_{LS}	relative humidity at the leaf surface
J_{max}	maximum rate of electron transport
K_s	soil water conductivity
K_{rad}	total conductivity in the root system in the radial direction
$K_{r_i}^R$	root conductivity in species i in the radial direction, obtained for each layer from K_{rad} according to the root distribution [*Amenu and Kumar*, 2008]
K_{ax}	total conductivity in the root system in the axial direction
$K_{r_i}^A$	root conductivity in species i in the axial direction, obtained for each layer from K_{ax} according to the root distribution [*Amenu and Kumar*, 2008]

LE_L	latent heat emitted from the litter layer to the atmosphere
LE_{eco}	latent heat emitted from the total ecosystem
LE_{shrubs}	latent heat emitted from the shrubs
LE_{PP}	latent heat emitted from ponderosa pine, PP
L_v	specific heat of vaporization
m	Ball Berry SLOPE
q_{s1}	air specific humidity in the soil in the top most layer
q_{a1}	air specific humidity in the atmosphere in the closest layer to surface
r_a	aerodynamic resistance
r_s	additional resistance of litter layer to transport of vapor
R_w	gas constant for water vapor
RH_{Ln}	relative humidity in the litter layer
s_f	sensitivity parameter, Tuzet model
T_L	temperature in the litter layer
T_{LSS}	temperature at the litter-atmosphere interface
T_{Ln}	temperature at the center of the litter layer
T_{SL}	temperature at the litter-soil interface
T_{s1}	soil temperature in the first (top most) layer
T_{a1}	temperature in the atmosphere in the layer closest to the surface
TC_L	thermal conductivity of the litter
TC_{s1}	soil thermal conductivity in the top most layer
V_{cmax}	maximum carboxylation velocity
α_L	litter thermal difussivity
θ	soil moisture
ψ_s	soil water potential
ψ_l	leaf water potential
ψ_f	reference water potential in the Tuzet-Ball-Berry model
ψ_{ri}	root water potential in *i*th vegetation species
ψ_L	litter water potential
ψ_{LL}	litter water potential for a liter moisture of $1\,kg\,kg^{-1}$ [*Ogee and Brunet*, 2002]
ψ_{Tr}	soil water potential threshold for hydraulic disconnection
$\overline{\psi_s}$	daily average soil water potential
$\rho_{b,L}$	litter bulk density [*Ogee and Brunet*, 2002]
Δz_L	litter layer thickness
Δz_{s1}	topsoil layer thickness
ρ_d	density of dry air
ρ_w	density of liquid water

[55] **Acknowledgments.** This research has been funded by NSF Grant ATM 06–28687 and EAR 09–11205. DTD was also supported by the National Science Foundation's International Research Fellowship Program (IRFP), award OISE-0900556. Fruitful discussions with Ciaran Harman are also acknowledged.

References

Ahn, H. K., T. J. Sauer, T. L. Richard, and T. D. Glanville (2009), Determination of thermal properties of composting bulking materials, *Bioresour. Technol.*, *100*(17), 3974–3981.

Alder, N. N., J. S. Sperry, and W. T. Pockman (1996), Root and stem xylem embolism, stomatal conductance, and leaf turgor in Acer grandidentatum populations along a soil moisture gradient, *Oecologia*, *105*(3), 293–301.

Allton, K., J. Harris, R. Rickson, and K. Ritz (2007), The effect of microbial communities on soil hydrological processes: A microcosm study utilising simulated rainfall, *Geoderma*, *142*(1–2), 11–17.

Amenu, G. G., and P. Kumar (2008), A model for hydraulic redistribution incorporating coupled soil-root moisture transport, *Hydrol. Earth Syst. Sci.*, *12*(1), 55–74.

Angers, D. A., and J. Caron (1998), Plant-induced changes in soil structure: Processes and feedbacks, *Biogeochemistry*, *42*(1), 55–72.

Ball, J., and J. Berry (1982), The ci/cs ratio: A basis for predicting stomatal control of photosynthesis, *Carnegie Inst. Washington Yearb.*, *81*, 88–92.

Bardgett, R., and D. Wardle (2010), *Aboveground-Belowground Linkages: Biotic Interactions, Ecosystem Processes, and Global Change*, pp. 481–492, Oxford Univ. Press, New York.

Bavel, C. H. M. V., and D. I. Hillel (1976), Calculating potential and actual Evaporation from a bare soil surface by simulation of concurrent flow water and heat, *Agric. Meteorol.*, *17*, 453–476.

Bernacchi, C. J., C. Pimentel, and S. P. Long (2003), In vivo temperature response functions of parameters required to model rubp-limited photosynthesis, *Plant Cell Environ.*, *26*(9), 1419–1430.

Bernacchi, C. J., P. B. Morgan, D. R. Ort, and S. P. Long (2005), The growth of soybean under free air [CO(2)] enrichment (FACE) stimulates photosynthesis while decreasing in vivo Rubisco capacity, *Planta*, *220*(3), 434–446.

Black, T. A., and J. Harden (1995), Effect of timber harvest on soil carbon at blodgett experimental forest, California, *Can. J. For. Res.*, *25*, 1385–1396.

Bleby, T. M., A. J. McElrone, and R. B. Jackson (2010), Water uptake and hydraulic redistribution across large woody root systems to 20 m depth, *Plant Cell Environ.*, *33*(20), 2132–2148.

Blizzard, W. E. (1980), Comparative resistance of the soil and the plant to water transport, *Plant Physiol.*, *66*(5), 809–814.

Bristow, K. L., G. S. Campbell, R. I. Papendick, and L. F. Elliott (1986), Simulation of heat and moisture transfer through a surface residue-soil system, *Agric. For. Meteorol.*, *36*, 193–214.

Brooks, J. R., F. C. Meinzer, R. Coulombe, and J. Gregg (2002), Hydraulic redistribution of soil water during summer drought in two contrasting pacific northwest coniferous forest, *Tree Physiol.*, *22*, 1107–1117.

Brooks, J. R., F. C. Meinzer, J. M. Warren, J. C. Domec, and R. Coulombe (2006), Hydraulic redistribution in a Douglas-fir forest: Lessons from system manipulations, *Plant Cell Environ.*, *29*(1), 138–150.

Burgess, S. S. O., M. A. Adams, N. C. Turner, and C. K. Ong (1998), The redistribution of soil water by tree root systems, *Oecologia*, *115*(3), 306–311.

Burgess, S. S. O., J. S. Pate, M. A. Adams, and T. E. Dawson (2000), Seasonal water acquisition and redistribution in the Australian woody phreatophyte, banksia prionotes, *Ann. Botany*, *85*(2), 215–224.

Burgess, S. S. O., M. A. Adams, N. C. Turner, D. A. White, and C. K. Ong (2001), Tree roots: Conduits for deep recharge of soil water, *Oecologia*, *126*(2), 158–165.

Bussiere, F., and P. Cellier (1994), Modification of the soil temperature and water content regimes by a crop residue mulch: Experiment and modeling, *Agric. For. Meteorol.*, *68*(1–2), 1–28.

Caldwell, M. M., and J. H. Manwaring (1994), Hydraulic lift and soil nutrient heterogeneity, *Nat. Resour. Res.*, *42*, 321–330.

Caldwell, M. M., and J. H. Richards (1989), Hydraulic lift—Water efflux from upper roots improves effectiveness of water-uptake by deep roots, *Oecologia*, *79*(1), 1–5.

Caldwell, M. M., T. E. Dawson, and J. H. Richards (1998), Hydraulic lift: Consequences of water efflux from the roots of plants, *Oecologia*, *113*(2), 151–161.

Campbell, G., and D. Norman (1998), *An Introduction to Environmental Biophysics*, Springer, New York.

Chung, S. O., and R. Horton (1987), Soil heat and water-flow with a partial surface mulch, *Water Resour. Res.*, *23*(12), 2175–2186.

Coops, N. C., T. Hilker, M. A. Wulder, B. St-Onge, G. Newnham, A. Siggins, and J. A. Trofymow (2007), Estimating canopy structure of Douglas-fir forest stands from discrete-return lidar, *Trees Struct. Funct.*, *21*(3), 295–310.

Dawson, T. E. (1993), Hydraulic lift and water use by plants. Implications for water balance, performance and plant-plant interactions, *Oecologia*, *95*(4), 565–574.

Dawson, T. E. (1996), Determining water use by trees and forests from isotopic, energy balance and transpiration analyses: The roles of tree size and hydraulic lift, *Tree Physiol.*, *16*(1–2), 263–272.

Domec, J.-C., J. M. Warren, F. C. Meinzer, J. R. Brooks, and R. Coulombe (2004), Native root xylem embolism and stomatal closure in stands of Douglas-fir and ponderosa pine: Mitigation by hydraulic redistribution, *Oecologia*, *141*(1), 7–16.

Domec, J.-C., J. S. King, A. Noormets, E. Treasure, M. J. Gavazzi, G. Sun, and S. G. McNulty (2010), Hydraulic redistribution of soil water by roots affects whole-stand evapotranspiration and net ecosystem carbon exchange, *New Phytol.*, *187*(1), 171–183, doi:10.1111/j.1469-8137.2010.03245.x.

Drewry, D. T., P. Kumar, S. Long, C. Bernacchi, X.-Z. Liang, and M. Sivapalan (2010a), Ecohydrological responses of dense canopies to environmental variability: 1. Interplay between vertical structure and photosynthetic pathway, *J. Geophys. Res.*, *115*, G04022, doi:10.1029/2010JG001340.

Drewry, D. T., P. Kumar, S. Long, C. Bernacchi, X.-Z. Liang, and M. Sivapalan (2010b), Ecohydrological responses of dense canopies to environmental variability: 2. Role of acclimation under elevated CO_2, *J. Geophys. Res.*, *115*, G04023, doi:10.1029/2010JG001341.

Emerman, S. H., and T. E. Dawson (1996), Hydraulic lift and its influence on the water content of the rhizosphere: An example from sugar maple, acer saccharum, *Oecologia*, *108*(2), 273–278.

Espeleta, J. F., J. B. West, and L. A. Donovan (2004), Species-specific patterns of hydraulic lift in co-occurring adult trees and grasses in a sandhill community, *Oecologia*, *138*(3), 341–349.

Farquhar, G. D., S. V. Caemmerer, and J. A. Berry (1980), A biochemical-model of photosynthetic CO_2 assimilation in leaves of c-3 species, *Planta*, *149*(1), 78–90.

Fisher, J. B., T. A. DeBiase, Y. Qi, M. Xu, and A. H. Goldstein (2005), Evapotranspiration models compared on a Sierra Nevada forest ecosystem, *Environ. Modell. Software*, *20*(6), 783–796.

Fisher, J. B., D. D. Baldocchi, L. Misson, T. E. Dawson, and A. H. Goldstein (2007), What the towers don't see at night: Nocturnal sap flow in trees and shrubs at two ameriflux sites in California, *Tree Physiol.*, *27*(4), 597–610.

Goldstein, A. H., N. E. Hultman, J. M. Fracheboud, M. R. Bauer, J. A. Panek, M. Xu, Y. Qi, A. B. Guenther, and W. Baugh (2000), Effects of climate variability on the carbon dioxide, water, and sensible heat fluxes above a ponderosa pine plantation in the Sierra Nevada (CA), *Agric. For. Meteorol.*, *101*(2–3), 113–129.

Haverd, V., and M. Cuntz (2010), Soil-litter-iso: A one-dimensional model for coupled transport of heat, water and stable isotopes in soil with a litter layer and root extraction, *J. Hydrol.*, *388*(3–4), 438–455.

Horton, J. L., and S. C. Hart (1998), Hydraulic lift: A potentially important ecosystem process, *Trends Ecol. Evol.*, *13*(6), 232–235.

Huang, B. G., and P. S. Nobel (1994), Root hydraulic conductivity and its components, with emphasis on desert succulents, *Agron. J.*, *86*(5), 767–774.

Hultine, K. R., W. L. Cable, S. S. O. Burgess, and D. G. Williams (2003), Hydraulic redistribution by deep roots of a chihuahuan desert phreatophyte, *Tree Physiol.*, *23*(5), 353–360.

Hultine, K. R., R. L. Scott, W. L. Cable, D. C. Goodrich, and D. G. Williams (2004), Hydraulic redistribution by a dominant, warm-desert phreatophyte: seasonal patterns and response to precipitation pulses, *Funct. Ecol.*, *18*(4), 530–538.

Huxman, T. E., K. A. Snyder, D. Tissue, A. J. Leffler, K. Ogle, W. T. Pockman, D. R. Sandquist, D. L. Potts, and S. Schwinning (2004), Precipitation pulses and carbon fluxes in semiarid and arid ecosystems, *Oecologia*, *141*(2), 254–268.

Ishikawa, C. M., and C. S. Bledsoe (2000), Seasonal and diurnal patterns of soil water potential in the rhizosphere of blue oaks: Evidence for hydraulic lift, *Oecologia*, *125*, 459–465.

Jackson, R. B., H. A. Mooney, and E. D. Schulze (1997), A global budget for fine root biomass, surface area, and nutrient contents, *Proc. Natl. Acad. Sci. U.S. A.*, *94*(14), 7362–7366.

Jackson, R. B., J. S. Sperry, and T. E. Dawson (2000), Root water uptake and transport: Using physiological processes in global predictions, *Trends Plant Sci.*, *5*(11), 482–488.

Katul, G. G., L. Mahrt, D. Poggi, and C. Sanz (2004), One- and two-equation models for canopy turbulence, *Boundary Layer Meteorol.*, *113*(1), 81–109.

Kramer, P. (1933), The intake of water through dead root systems and its relation to the problem of absorption by transpiring plants, *Am. J. Botany*, *20*(7), 481–492.

Kumar, P. (2011), Typology of hydrologic predictability, *Water Resour. Res.*, *47*, W00H05, doi:10.1029/2010WR009769.

Kurpius, M. R., J. A. Panek, N. T. Nikolov, M. McKay, and A. H. Goldstein (2003), Partitioning of water flux in a Sierra Nevada ponderosa pine plantation, *Agric. For. Meteorol.*, *117*(3–4), 173–192.

Lee, J. E., R. S. Oliveira, T. E. Dawson, and I. Fung (2005), Root functioning modifies seasonal climate, *Proc. Natl. Acad. Sci. U. S. A.*, *102*(49), 17,576–17,581.

Ludwig, F., T. E. Dawson, H. Kroon, F. Berendse, and H. H. T. Prins (2003), Hydraulic lift in acacia tortilis trees on an east African savanna, *Oecologia*, *134*(3), 293–300.

Ludwig, F., T. E. Dawson, H. H. T. Prins, F. Berendse, and H. Kroon (2004), Below-ground competition between trees and grasses may overwhelm the facilitative effects of hydraulic lift, *Ecol. Lett.*, *7*(8), 623–631.

McCulley, R. L., E. G. Jobbágy, W. T. Pockman, and R. B. Jackson (2004), Nutrient uptake as a contributing explanation for deep rooting in arid and semi-arid ecosystems, *Oecologia*, *141*(4), 620–628.

Meinzer, F. C., J. R. Brooks, S. Bucci, G. Goldstein, F. G. Scholz, and J. M. Warren (2004), Converging patterns of uptake and hydraulic redistribution of soil water in contrasting woody vegetation types, *Tree Physiol.*, *24*(8), 919–928.

Mendel, M., S. Hergarten, and H. J. Neugebauer (2002), On a better understanding of hydraulic lift: A numerical study, *Water Resour. Res.*, *38*(10), 1183, doi:10.1029/2001WR000911.

Misson, L., J. A. Panek, and A. H. Goldstein (2004), A comparison of three approaches to modeling leaf gas exchange in annually drought-stressed ponderosa pine forests, *Tree Physiol.*, *24*(5), 529–541.

Misson, L., J. W. Tang, M. Xu, M. McKay, and A. Goldstein (2005), Influences of recovery from clear-cut, climate variability, and thinning on the carbon balance of a young ponderosa pine plantation, *Agric. For. Meteorol.*, *130*(3–4), 207–222.

Misson, L., K. P. Tu, R. A. Boniello, and A. H. Goldstein (2006), Seasonality of photosynthetic parameters in a multi-specific and vertically complex forest ecosystem in the Sierra Nevada of California, *Tree Physiol.*, *26*(6), 729–741.

Moreira, M. Z., F. G. Scholz, S. J. Bucci, L. S. Sternberg, G. Goldstein, F. C. Meinzer, and A. C. Franco (2003), Hydraulic lift in a neotropical savanna, *Funct. Ecol.*, *17*(5), 573–581.

Muñoz, M., F. Squeo, M. León, Y. Tracol, and J. Gutiérrez (2008), Hydraulic lift in three shrub species from the Chilean coastal desert, *J. Arid Environ.*, *72*(5), 624–632.

Nadezhdina, N., T. S. David, J. S. David, M. I. Ferreira, M. Dohnal, M. Tesa, K. Gartner, E. Leitgeb, and V. Nadezhdin (2010), Trees never rest: The multiple facets of hydraulic redistribution, *Library*, *444*, 431–444, doi:10.1002/eco.

Nikolov, N. (1995), Coupling biochemical and biophysical processes at the leaf level: An equilibrium photosynthesis model for leaves of C3 plants, *Ecol. Modell.*, *80*(2–3), 205–235.

Nye, P., and P. Tinker (1977), *Solute Movement in the Soil-Root System*, Univ. of Calif. Press, Berkeley, Calif.

Oakley, B. B., M. P. North, and J. F. Franklin (2003), The effects of fire on soil nitrogen associated with patches of the actinorhizal shrub *ceanothus cordulatus, Plant Soil*, *254*(1), 35–46.

Ogee, J., and Y. Brunet (2002), A forest floor model for heat and moisture including a litter layer, *J. Hydrol.*, *255*(1–4), 212–233.

Panek, J. A. (2004), Ozone uptake, water loss and carbon exchange dynamics in annually drought-stressed pinus ponderosa forests: Measured trends and parameters for uptake modeling, *Tree Physiol.*, *24*(3), 277–290.

Park, H.-T., S. Hattori, and T. Tanaka (1998), Development of a numerical model for evaluating the effect of litter layer on evaporation, *J. For. Res.*, *3*(1), 25–33.

Peterson, P. (1975), *Native Trees of the Sierra Nevada, Calif. Nat. History Guides*, 91 pp., Univ. of California, Berkeley, Calif.

Plamboeck, A. H., M. North, and T. E. Dawson (2008), Conifer seedling survival under closed-canopy and manzanita patches in the Sierra Nevada, *Madroño*, *55*(3), 193–203.

Pregitzer, K. S., R. L. Hendrick, R. Fogel, and L. Hendrick (1993), The demography of fine roots in response to patches of water and nitrogen, *New Phytol.*, *125*, 575–580.

Prieto, I., K. Martínez-Tillería, L. Martínez-Manchego, S. Montecinos, F. I. Pugnaire, and F. A. Squeo (2010), Hydraulic lift through transpiration suppression in shrubs from two arid ecosystems: patterns and control mechanisms, *Oecologia*, *163*(4), 855–865.

Querejeta, J., L. Egerton-Warburton, and M. Allen (2007), Hydraulic lift may buffer rhizosphere hyphae against the negative effects of severe soil drying in a California Oak savanna, *Soil Biol. Biochem.*, *39*(2), 409–417.

Richards, J. H., and M. M. Caldwell (1987), Hydraulic lift—Substantial nocturnal water transport between soil layers by artemisia-tridentata roots, *Oecologia*, *73*(4), 486–489.

Rose, K. L., R. C. Graham, and D. R. Parker (2003), Water source utilization by *Pinus jeffreyi* and *Arctostaphylos patula* on thin soils over bedrock, *Oecologia*, *134*(1), 46–54.

Ryel, R. J., M. M. Caldwell, C. K. Yoder, D. Or, and A. J. Leffler (2002), Hydraulic redistribution in a stand of artemisia tridentata: evaluation of benefits to transpiration assessed with a simulation model, *Oecologia*, *130*(2), 173–184.

Schaap, M. G., W. Bouten, and J. M. Verstraten (1997), Forest floor water content dynamics in a Douglas fir stand, *J. Hydrol.*, *201*(1–4), 367–383.

Schade, G. W. (2002), Plant physiological influences on the fluxes of oxygenated volatile organic compounds from ponderosa pine trees, *J. Geophys. Res.*, *107*(D10), 4082, doi:10.1029/2001JD000532.

Schenk, H. J., and R. B. Jackson (2002), The global biogeography of roots, *Ecol. Monogr.*, *72*(3), 311–328.

Scholz, F. G., S. J. Bucci, G. Goldstein, F. C. Meinzer, and A. C. Franco (2002), Hydraulic redistribution of soil water by neotropical savanna trees, *Tree Physiol.*, *22*(9), 603–612.

Schulze, E. D., M. M. Caldwell, J. Canadell, H. A. Mooney, R. B. Jackson, D. Parson, R. Scholes, O. E. Sala, and P. Trimborn (1998), Downward flux of water through roots (i.e., inverse hydraulic lift) in dry Kalahari sand, *Oecologia*, *115*(4), 460–462.

Scott, R. L., W. L. Cable, and K. R. Hultine (2008), The ecohydrologic significance of hydraulic redistribution in a semiarid savanna, *Water Resour. Res.*, *44*, W02440, doi:10.1029/2007WR006149.

Smith, D. M., N. A. Jackson, J. M. Roberts, and C. K. Ong (1999), Reverse flow of sap in tree roots and downward siphoning of water by grevillea robusta, *Funct. Ecol.*, *13*(2), 256–264.

Smith, S. G. (2005), Effects of moisture on combustion characteristics of live California chaparral and Utah foliage, Master's thesis, Brigham Young Univ., Provo, Utah.

Tang, J. W., L. Misson, A. Gershenson, W. X. Cheng, and A. H. Goldstein (2005), Continuous measurements of soil respiration with and without roots in a ponderosa pine plantation in the Sierra Nevada mountains, *Agric. For. Meteorol.*, *132*(3–4), 212–227.

Tuzet, A., A. Perrier, and R. Leuning (2003), A coupled model of stomatal conductance, photosynthesis and transpiration, *Plant Cell Environ.*, *26*(7), 1097–1116.

Tyree, M. T., and J. S. Sperry (1988), Do woody plants operate near the point of catastrophic xylem dysfunction caused by dynamic water stress?: Answers from a model, *Plant Physiol.*, *88*(3), 574–580.

Wang, G. (2011), Assessing the potential hydrological impacts of hydraulic redistribution in Amazonia using a numerical modeling approach, *Water Resour. Res.*, *47*, W02528, doi:10.1029/2010WR009601.

Wang, G., C. Alo, R. Mei, and S. Sun (2010), Droughts, hydraulic redistribution, and their impact on vegetation composition in the Amazon forest, *Plant Ecol.*, *212*(4), 663–673, doi:10.1007/s11258-010-9860-4.

Warren, J. M., F. C. Meinzer, J. R. Brooks, J. C. Domec, and R. Coulombe (2007), Hydraulic redistribution of soil water in two old-growth coniferous forests: Quantifying patterns and controls, *New Phytol.*, *173*(4), 753–765.

Warren, J. M., J. R. Brooks, M. I. Dragila, and F. C. Meinzer (2011), In situ separation of root hydraulic redistribution of soil water from liquid and vapor transport, *Oecologia*, *166*(4), 899–911.

Wilson, K. (2000), Factors controlling evaporation and energy partitioning beneath a deciduous forest over an annual cycle, *Agric. For. Meteorol.*, *102*(2–3), 83–103.

Wright, H., and A. Bailey (1982), *Fire Ecology, United States and Southern Canada, Classics Ecol. Environ. Sci.*, 229 pp., Wiley, New York.

Xu, M., and Y. Qi (2001), Soil-surface CO_2 efflux and its spatial and temporal variations in a young ponderosa pine plantation in Northern California, *Global Change Biol.*, *7*(6), 667–677.

Yoder, C. K., and R. S. Nowak (1999), Hydraulic lift among native plant species in the Mojave desert, *Plant Soil*, *215*(1), 93–102.

Zou, C. B., P. W. Barnes, S. Archer, and C. R. McMurtry (2005), Soil moisture redistribution as a mechanism of facilitation in savanna tree-shrub clusters, *Oecologia*, *145*(1), 32–40.

D. T. Drewry, Jet Propulsion Laboratory, California Institute of Technology, 4800 Oak Grove Dr., Pasadena, CA 91109, USA. (drewryd@gmail.com)

A. H. Goldstein, Department of Environmental Science, Policy, and Management, University of California at Berkeley, 330 Hilgard Hall, Berkeley, CA 94720, USA. (ahg@berkeley.edu)

P. Kumar and J. C. Quijano, Department of Civil and Environmental Engineering, University of Illinois at Urbana-Champaign, 205 N. Mathews Ave., Office 2527B, Urbana, IL 61801, USA. (kumar1@illinois.edu; quijano2@illinois.edu)